February 4, 1977

Final Report, 76-2
December 5, 1975, to December 4, 1976

STRUCTURE/PROPERTY CORRELATIONS IN PRIMARY EXPLOSIVES

By: Craig M. Tarver, Thomas C. Goodale,
    Michael Cowperthwaite, and Marion E. Hill

Prepared for:

U.S. NAVAL SEA SYSTEMS COMMAND
Explosives and Pyrotechnics Branch, SEA 0332
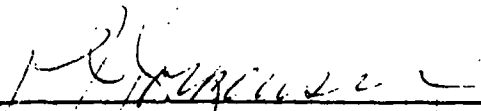Washington, D.C. 20300

Attn: Dr. A. B. Amster

D D C
SEP 28 1977
C

Project Serial Number SF3354-317
NAVSEASYSCOM Contract Number N00024-76-C-5329

SRI Project No. PYU-4770   8 S... 1977

Approved by:

P. J. Jorgensen, Vice President
Physical and Life Sciences Group   1581

STANFORD RESEARCH INSTITUTE
Menlo Park, California 94025 · U.S.A.

1581

REPORT DOCUMENTATION PAGE		READ INSTRUCTIONS BEFORE COMPLETING FORM
1. REPORT NUMBER	2. GOVT ACCESSION NO.	3. RECIPIENT'S CATALOG NUMBER
4. TITLE (and Subtitle) Structure Property Correlations in Primary Explosives		5. TYPE OF REPORT & PERIOD COVERED Final December 5, 1975, to December 4, 1976
		6. PERFORMING ORG. REPORT NUMBER 76-2
7. AUTHOR(s) Craig M. Tarver, Michael Cowperthwaite, Thomas C. Goodale, and Marion E. Hill		8. CONTRACT OR GRANT NUMBER(s) N00024-76-C-5329
9. PERFORMING ORGANIZATION NAME AND ADDRESS SRI International (formerly Stanford Research Institute) 333 Ravenswood Avenue Menlo Park, CA 94025		10. PROGRAM ELEMENT, PROJECT, TASK AREA & WORK UNIT NUMBERS Serial No. SF3354-316
11. CONTROLLING OFFICE NAME AND ADDRESS U.S. Naval Sea Systems Command Explosives and Pyrotechnics Branch, SEA 0332 Washington, D. C. 20300		12. REPORT DATE Feb. 4, 1977
		13. NO. OF PAGES 86
14. MONITORING AGENCY NAME & ADDRESS (if diff. from Controlling Office) N. A.		15. SECURITY CLASS. (of this report) Unclassified
		15a. DECLASSIFICATION/DOWNGRADING SCHEDULE

16. DISTRIBUTION STATEMENT (of this report)

DISTRIBUTION STATEMENT A
Approved for public release;
Distribution Unlimited

17. DISTRIBUTION STATEMENT (of the abstract entered in Block 20, if different from report)

18. SUPPLEMENTARY NOTES

19. KEY WORDS (Continue on reverse side if necessary and identify by block number)

Primary Explosives
Deflagration Detonation Transition
Sensitivity
Explosive Structure/Property
1-Methyl-5-Nitrotetrazole

2-Methyl-5-Nitrotetrazole
Cast Explosives
Explosive Salts
Explosive Covalent Compounds

20. ABSTRACT (Continue on reverse side if necessary and identify by block number)

The objective of this study was to identify the characteristics of primary explosives that account for their action as primaries by correlating their physical and chemical properties with their molecular structures. It was found that molecular structure could be correlated with properties within classes in a qualitative sense; however, quantitative data such as heats of formation and bond energies must still be developed before a firm scientific base can be established for designing molecular structure and

DD FORM 1473 1 JAN 73
EDITION OF 1 NOV 65 IS OBSOLETE

19. KEY WORDS (Continued)

20 ABSTRACT (Continued)

predicting properties, as is possible for secondary explosives.

Essential primary explosive properties are the ability to remain ignited and quickly undergo deflagration to detonation transition (DDT). Several practical primaries such as lead styphnate and lead azide have detectable burn times before detonation. Thus the study of DDT in cast explosives was initiated to establish whether DDT measurements were useful as a method to screen explosives for primary properties. DDT studies of two potential castable primaries, the isomers 1-methyl-5-nitrotetrazole (1-MNT) and 2-methyl-5-nitrotetrazole (2-MNT) were undertaken as a first step to achieving this objective.

Our experiments showed that DDT occurs more readily in cast 2-MNT than in cast 1-MNT. The threshold voltages for ignition by hot bridgewire were found to be 110 volts for cast 2-MNT and 375 volts for cast 1-MNT. Critical times and distances for DDT in cast 2-MNT of 8 μsec and 2-3 mm, respectively, were determined by performing experiments on charges of different lengths. Critical parameters for cast 1-MNT were not determined because the threshold voltage for ignition was too high.

Macek's model for DDT in cast explosives was modified in a theoretical study to provide a more realistic treatment of the accelerating flame. Calculations were made with the deflagration treated as a reactivity discontinuity whose burnt state satisfied either Chapman-Jouguet (CJ) condition or the condition of zero particle velocity to determine upper and lower limits for the deflagration velocity as functions of pressure in the unburned explosive. Times and distances for DDT in cast pentolite and crystalline lead azide were predicted and agreed well with the meager experimental data available.

DD FORM **1473** (BACK)
1 JAN 73
EDITION OF 1 NOV 65 IS OBSOLETE

February 4, 1977

Final Report, 76-2
December 5, 1975, to December 4, 1976

STRUCTURE/PROPERTY CORRELATIONS IN PRIMARY EXPLOSIVES

By: Craig M. Tarver, Thomas C. Goodale,
    Michael Cowperthwaite, and Marion E. Hill
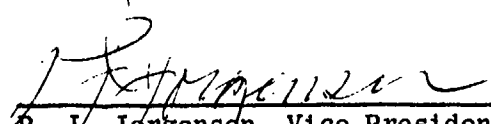
Prepared for:

U.S. NAVAL SEA SYSTEMS COMMAND
Explosives and Pyrotechnics Branch, SEA 0332
Washington, D.C. 20300

Attn: Dr. A. B. Amster

Project Serial Number SF3354-317
NAVSEASYSCOM Contract Number N00024-76-C5329

SRI Project No. PYU-4770

Approved by:

P. J. Jorgensen, Vice President
Physical and Life Sciences Group

CONTENTS

FOREWORD

This final report is submitted in fulfillment of Contract N00024-76-C-5329, Navy Project Serial Number SF3354-316, and covers the period December 5, 1975 through December 4, 1976. For completeness, summaries and excerpts are included from the previous two contracts on the same subject, Contract N00017-73-C-4346 and Contract N00024-75-C-5008.

The research program was performed by staff of the Physical Sciences Division under the supervision of Marion E. Hill. Craig M. Tarver and Thomas C. Goodale were the principal experimentalists, and Michael Cowperthwaite with Craig Tarver developed the modified theory of deflagration to detonation transition.

We wish to acknowledge the extensive and helpful discussions and suggestions by our monitors, Dr. A. B. Amster, Head, Explosives and Pyrotechnics Branch, SEA 0332, and Mr. Irving Kabik of the White Oak Laboratory, Naval Surface Weapons Center.

ILLUSTRATIONS

TABLES

I INTRODUCTION AND SUMMARY

Primary explosives such as lead azide have been used for nearly a hundred years to initiate detonation of less sensitive secondary explosives such as TNT. Today lead azide is the principal primary explosive used by the Department of Defense. Because of several deficiencies with lead azide, notably its unpredictable sensitivity often arising from copper azide formation, many other energetic materials have been prepared for the same purposes, but most have failed to find general acceptance in the explosives community for one reason or another.

Consequently, there are recurrent requests for new primaries that are not in the azide class. Often an approach to fulfilling the need is to search the shelves for any explosive that one suspects is so highly sensitive that it may be a primary. Such an approach leads inevitably to an Edisonian try-and-see series of syntheses and tests. The continuing use of lead azide indicates that no other single compound has been found to fulfill all requirements.

Too little is known of the influence of chemical structure in a fundamental way on the action of initiators. In the secondary explosive field, much research has been conducted with the result that some correlation between chemical structure and detonation behavior is available to assist chemists and physicists in designing and applying new secondary systems. Such is not the case in the primary field, which has experimental results and some empirical correlations, but as yet no general theoretical basis.

The objective of this research was, therefore, to place the choice of primary explosives for practical applications on a firmer theoretical

base related to the chemical and physical properties of those materials whose action is generally classed as "primariness." This base then should permit reasonable correlation between structure and primary properties, and eventually lead to the design of explosive molecules suitable for synthesis and testing in practical detonation compositions. Replacement of lead azide without an Edisonian hit-or-miss approach would be feasible.

Our emphasis was placed on obtaining as much information as possible on compounds other than azides since this class has had extensive study and development. (A review on inorganic azides in two volumes is being published by Picatinny Arsenal.[1]) Attempts to synthesize new primary explosives have concentrated on variations of metal derivatives of energetic compounds, for example, heavy metal compounds such as lead styphnate and silver azide or azo compounds such as diazodinitrophenol, tetracene and cyanuric triazide. Although several of these materials also find use as primaries, their applications are limited and they are often used in conjunction with lead azide. No fully organic primaries are used at this time.

The very special requirements for efficient primaries--sensitive but not too sensitive, fast transition from deflagration to detonation, high energy yield, and reproducible properties when prepared in production quantities--place considerable constraints on design and testing of initiators. Guidelines for preparing new materials to meet stringent requirements for useful primary explosives are based largely on experience with materials that work rather than on any fundamental principles of kinetics, thermochemistry, and physics. We believe that this was an opportune time to attempt the characterization of primary explosives in a more fundamental way than had been possible in the past and, on the basis of these relationships, to develop new superior materials and ways of testing and evaluating them.

Numerous research workers in the field of explosives were interviewed to determine the state of the art and to identify the major unsolved problems in applications of primaries. As a complement to these visits, we examined the literature for gaps in knowledge. Another task was an attempt to correlate the physical and chemical properties of explosives with their action as primaries. The results were not quantitative and provided only several general observations and conclusions from which an approach to a possible screening method was derived.

It seems much easier to compare a primary explosive with a secondary explosive than to define a primary explosive in absolute terms. Primary and secondary explosives have many similarities. Both will burn to detonation, although secondaries sometimes go out; primaries never do. Confinement and a "long" burning time are required for secondaries. The existence of "near primaries" such as some of the hydroxynitroaromatic compounds and "sensitive" secondaries like PETN are suggestive of many other compounds that exist between the main body of primaries and the main body of secondaries. However, these have received relatively little attention because there is no obvious practical use for them. Summarizing from a physico-chemical point of view, primaries and secondaries differ in degree rather than in kind.

The most important properties of a primary explosive are the ability to remain ignited and the ability to undergo very fast deflagration to detonation transition (DDT). These ignition properties are a primary's strength and its weakness. It is a strength because the function of a primary is to detonate on being ignited: all other things being equal, the faster the DDT, the better the primary. It is a weakness because accidental initiation of deflagration will also result in detonation.

3

Because DDT seemed to be a distinguishing characteristic that could be measured, an experimental program was designed to test whether DDT measurements could be used as a definitive screening technique. This research program was based on the following assumptions:

(1) An important measurable distinction between a primary and a secondary explosive is that a primary explosive undergoes very much faster deflagration to detonation transition (DDT).

(2) The difference between primaries and secondaries is one of degree rather than kind; therefore, experience obtained in measuring DDT in secondaries can be applied to primaries.

(3) It would be easier to develop a quantitative model for DDT in cast explosives than in porous explosives.

DDT studies of two potential isomeric cast primaries, 1-methyl-5-nitrotetrazole (1-MNT) and 2-methyl-5-nitrotetrazole (2-MNT), were undertaken as the first step towards achieving this objective. Isomeric cast explosives are more convenient for isolating the effects of chemical structure in primaries because isomers have different molecular structures but essentially the same physical properties; because inhomogeneities leading to increased sensitivity are minimized by the casting process; and because the mechanism of DDT is more fully understood in cast explosives than in porous explosives.

Our experiments showed that DDT occurs more readily in cast 2-MNT than in cast 1-MNT, clearly demonstrating the influence of chemical structure on primary explosive behavior. The threshold voltages for ignition by a hot bridgewire were found to be 110 volts for cast 2-MNT and 375 volts for cast 1-MNT. Critical times and distances for DDT in cast 2-MNT of 8 μsec and 2-3 mm, respectively, were determined by performing experiments on charges of different lengths. The same critical parameters for cast 1-MNT were not determined, as will be explained later, because the threshold voltage for ignition was too high.

4

Macek's model for DDT in cast explosives was modified in the theoretical study to provide a more realistic treatment of the accelerating flame. Calculations were made with the deflagration treated as a reactive discontinuity whose burnt state satisfied either the Chapman-Jouguet (CJ) condition or the condition of zero particle velocity to determine upper and lower limits for the deflagration velocity as functions of pressure in the unburned explosive. Times and distances for DDT in cast pentolite and crystalline lead azide were predicted and agreed well with the meager experimental data available.

II STRUCTURAL CONSIDERATIONS

A. Structure-Property Characteristics

The objective of the first part of the general program[2] was to
survey the published literature to find correlatable characteristics
of primary compounds. Complementary to this effort, we interviewed a
number of research workers familiar with primary explosives to gather the
latest unpublished information on compounds other than azides under
development. Their views were also solicited on which aspects of research
were most needed to provide new candidate compounds for useful detonants.[*]

Emphasis in the survey and discussions was on compounds that were
generally considered "primaries" by their sensitivity characteristics
or usage. Table 1 lists thirteen general classes or families of compounds
and their principal energetic groupings. The literature was searched for
structure characteristics that may be a key to their "primariness;"
thermochemical properties such as heat of formation; reaction kinetics;
detonation properties, including detonation velocity, pressure, ease
of initiation by hot wire, deflagration to detonation information; and
physical properties of density, stability, sensitivity, crystal forms,
and related data.

The survey did not reveal a consistently measured property that
would allow a correlation in a broad sense for predictive purposes,
except for the commonly experienced sensitivity characteristics. The

---

[*]Not all compounds considered as primary explosives are useful as
initiators or detonants; the latter are those compounds that have passed
a number of practical tests and development in the practical configu-
ration of a detonator or fuze train. An expression sometimes heard is,
"A primary the compound may be, but a detonant it is not."

Table 1

CLASSES OF PRIMARY EXPLOSIVES
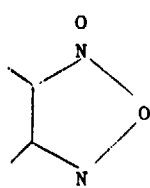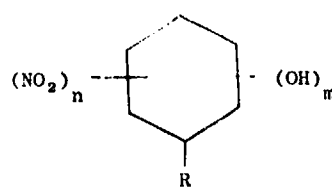
Classes, Energy Group	Salts	Covalent
Acetonitriles $-C - CN$	K-dinitroacetonile	Trinitroacetonitrile
Acetylides $-C \equiv CH$	Ag	Dicyanoacetylene
Azides $-N_3$	Pb, Ag, Cu, Th	Trinitrotriazidobenzene Cyanuric triazide
Fulminates $-NCO$	Hg, Ag, others	--
Furoxanes 	K dinitrobenzofuroxane	Benzotrifuroxan
Nitrocyanamides $-N(NO_2)CN$	Ag, Ba	Nitrocyanamide·H_2O
Nitroaromatics 	Pb Styphnate K, Ba, Trinitrophloro-glucinate K, Ba, Dinitrocatechol	Styphnic Acid Trinitrophloroglucinol Dinitrocatechol Diazodinitrophenol, $R=N_3$ Bis(difluoramino)hexa-nitrodiphenyl (FDIPAM), $R=NF_2$

7

Table 1 (Concluded)

CLASSES OF PRIMARY EXPLOSIVES

Classes, Energy Group	Salts	Covalent
Tetrazoles	R = H(Ag, Cu, Ni, Pb)	Tetrazole (unstable)
	R = NH$_2$(Ni, Co, Pb)	Tetrazene
	R = N$_3$(Ag, Na, K, Cd)	1-Methyl-5-nitrotetrazole
	R = NN-tetrazole(Hg, Tl, Na)	2-Methyl-5-nitrotetrazole
	R = Cl(Ag, Cu)	Azidotetrazole
	R = NH-NH-tetrazole(Na, Ag, Tl, Cu, Hg, Ni, Co, Pb)	
	R = CH$_3$(Ag, Cu, Pb)	
	R = Phenyl(Hg, Cu, Pb)	
	R = NHNO$_2$(Ag, Tl, K, Pb)	
	R = NO$_2$(Hg, Ag, Tl, Na, K, Cu, Hg(ic), Ni, Co, Pb)	
	R = NHNH$_2$(Ag, Tl, K, Cu, Ni, Co, Pb)	
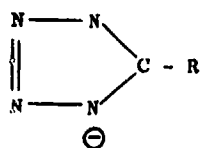
Perchlorate CP

$(ClO_4)_2$

$$X = N{-}N \diagdown C - CN$$
$$N{-}N \diagup$$
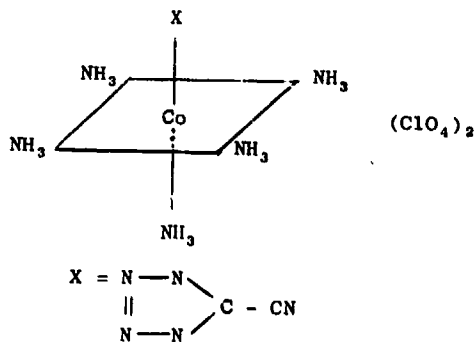
Miscellaneous

Nitrogen triiodide

Dinitrogentetrasulfide

Ag - methylene dinitramine

8

latter will for some time probably broadly define primary candidates
as being compounds easily ignited by low energy inputs from impact,
spark, hot wire, and shock. Most of the data that were even moderately
useful for correlation were usually within families of compounds.
There is a priori no basis at present for assuming primariness from
structure examination. However, one may identify energetic structural
elements in a given highly energetic family of compounds that would
forewarn one to look for primary characteristics.

For stability and ease of handling, the most used compounds are
the salts of highly sensitive covalent energetic compounds, such as
hydrazoic acid and the tetrazoles, and the salts of some less sensitive
secondary explosive compounds, such as styphnic acid. The inclusion of
azo linkages in a structure seems to impart primary sensitivity, especially
in the form of the azide group, $-N_3$, and in heterocyclic high nitrogen
compounds as represented by the triazole and tetrazole groups. Similar
unsaturate nitrogen linkages are represented by the fulminate NCO and
by the hetero furoxane in the "free" form, such as benzotrifuroxane (BTF)
or salt form, e.g., potassium dinitrobenzofuroxan. Other primary
candidates have come from nitrogen unsaturate compounds having combina-
tions of the above groups, as represented by the nitro furoxan and nitro
azido compounds; also in some cases the nitroamino group is combined with
an unsaturate group, as in a nitrocyanamide salt. Some exceptions to
this classification of generalities are the inorganic sensitive compounds
such as perchlorate salts. Also organic difluoramino compounds have
sensitivity characteristics that at least suggest they be considered.

Although most of the primaries in practical use as detonants are
salts, an increasing number of covalent, or "free acid," forms of
explosives are receiving attention. The compound, FDIPAM,[3] was recently
evaluated as a primary. It was found to be comparable to lead styphnate

9

in developing initiation to detonation and slightly less sensitive to initiation by hot wire than lead azide. ERDA is currently evaluating the compound, BTF, as an initiator. In our laboratories tests on 2-methyl-5-nitrotetrazole have indicated that it has a deflagration to detonation transition similar to lead azide; further study may be warranted. Other organic compounds that have been considered are trinitrotriazidobenzene, cyanuric triazide, and diazodinitrophenol; the last has use as an initiator in commercial compositions.

B. Structure-Property Correlations

1. Metal Ionization Potentials[2]

A few structure-property correlations have been suggested for primary explosives. One of the most interesting was proposed independently by Gray[4] and by Taylor and Jenkins[5] (GTJ). The GTJ postulate is that, within a family of explosive salts such as the azides or tetrazoles, the greater the ionization potential of the cation, the more likely the compound is a primary explosive. This concept may be useful for screening new families of salts. Since H and Ag have high ionization potentials, if the free acid or silver salt of a new family does not show primise, it is likely that other salts will not be useful. The basis of this correlation is probably the variation in heat of formation of the salt with the ionization potential of the cation.

For example, consider the azides. Azide thermochemistry is particularly simple because the main mode of decomposition is to the elements; therefore, the heat of detonation (an indicator of sensitivity) is simply the heat of formation for the metal azides,

$$AgN \rightarrow Ag + 3/2 \ N_2 + \Delta H_f(AgN_3)$$
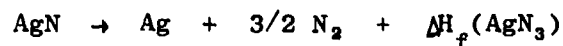
and for hydrogen azide,

$$HN_3 \rightarrow 1/2 \ H_2 + 3/2 \ N_2 + \Delta H_f(HN_3)$$

10
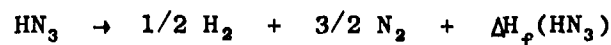
Figures 1 and 2 show that the heats of formation correlate well with the ionization potential of the metal. The ionization potential gives a quantitative measure of the degree of ionic character. It is interesting to note that ZnN_6 is significantly off the curve for divalent cations. Perhaps the heat of formation of ZnN_6 should be remeasured as the ionization potential is surely well known.

Although the GTJ postulate is useful for screening, the concept is limited because some exceptions occur and because it cannot be used outside the family of compounds. Furthermore, the heat of detonation is not the sole criterion for usefulness as a primary. TNT has a higher heat of detonation than lead azide.

2. Bond Rearrangement[2]

Roberts has postulated[6] that, for a compound to be a primary explosive, the structure should be capable of decomposing to products with rearrangement of the electrons (i.e., bonds) rather than the atoms. This is a stimulating idea and readily explains the fast DDT of the simple-molecule primaries like the azides, fulminates, and acetylides.

We selected two compounds for further study:

$$\begin{matrix} N = CH \\ | \quad\quad\quad \diagdown \\ \quad\quad\quad\quad C = O \\ | \quad\quad\quad \diagup \\ N = CH \end{matrix} \qquad and \qquad \begin{matrix} HC = N \\ | \quad\quad\quad \diagdown \\ \quad\quad\quad\quad C = O \\ | \quad\quad\quad \diagup \\ HC = N \end{matrix}$$

<div align="center">A   B</div>
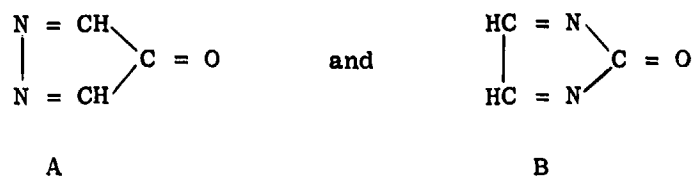
Both isomers formally dissociate with only electronic and not atomic rearrangement to 2HCN + CO. (There are no reports in the literature of synthesis of A or B and no new routes to A and B that seem reasonable.) Benson and Shaw have estimated[7] the heat of formation of A to be 43 $\pm$ 5 kcal/mole and of B to be 1 $\pm$ 5 kcal/mole.
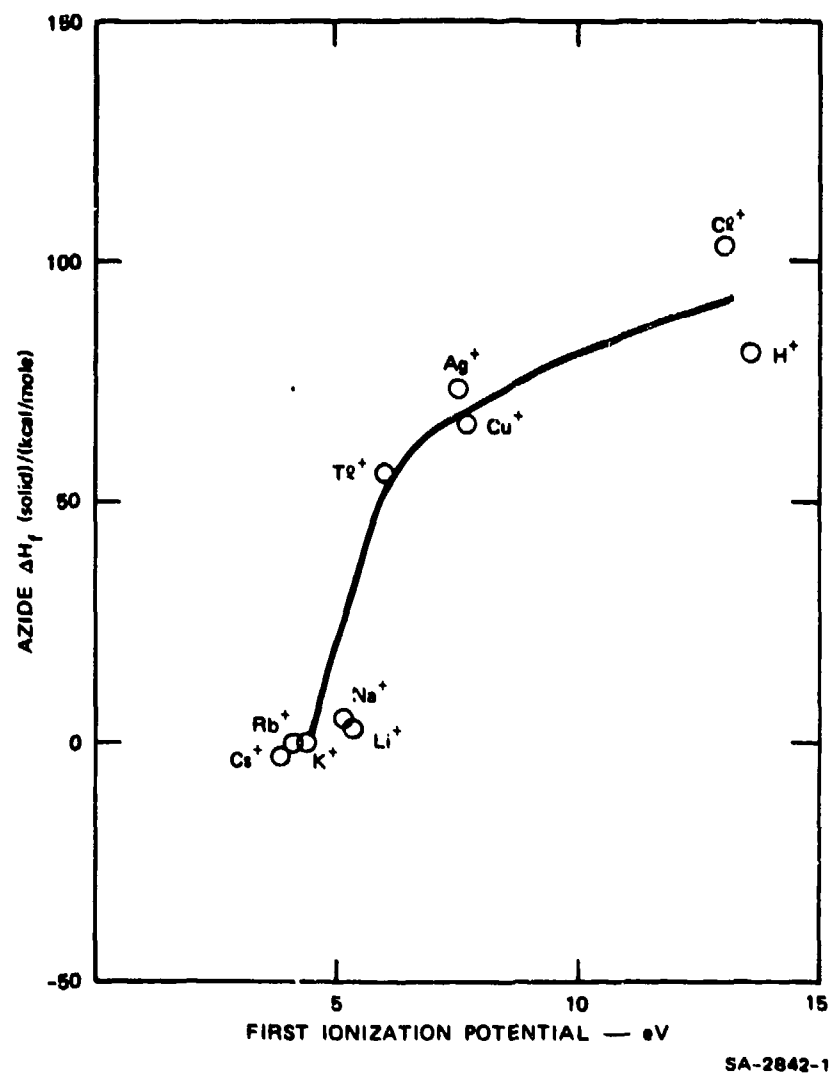
FIGURE 1   CORRELATION OF HEATS OF FORMATION IN THE SOLID STATE
OF MONOVALENT AZIDES WITH FIRST IONIZATION POTENTIAL OF
THE CATIONS
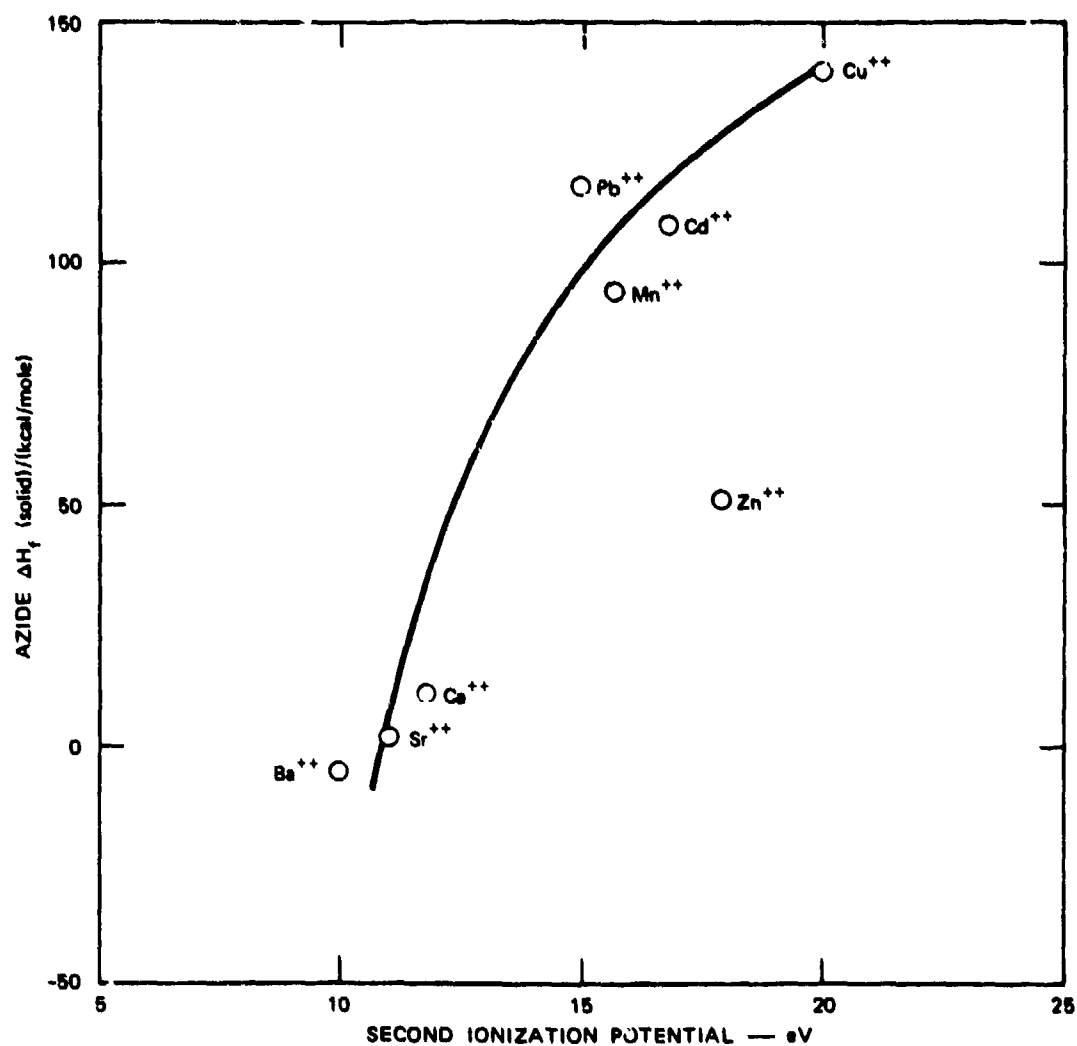
SA-2842-2

FIGURE 2   CORRELATION OF HEATS OF FORMATION IN THE SOLID STATE OF
DIVALENT AZIDES WITH SECOND IONIZATION POTENTIAL OF
THE CATIONS

The minimum rearrangement products for both A and B are 2HCN + CO. The sum of the heat of formation of the products is $(2 \times 32.3) - 26.4 = 38.2$ kcal/mole. Therefore, decomposition of A to 2HCN and CO would liberate 5 ± 5 kcal/mole, and decomposition of B to the same products would adsorb 37 ± 5 kcal/mole from the surroundings. Thus A is a marginal explosive, and B is unlikely to explode by electron rearrangement mechanism.

Another argument against the concept arises from examining the gas generator, $(-CH=N-N=CH-)_n$, prepared by Reed.[8] Benson and Shaw have estimated the heat of formation of the repeating unit to be 68 ± 5 kcal/mole. If the products are 2HCN, $(2 \times 32.3) - 64.6$ kcal/mole, the decomposition yields 3.4 kcal/mole, and if the products are CH≡CH (54.2 kcal/mole) + N_2 (0 kcal/mole). Reed found, consistent with these estimates, that the compounds indeed did not detonate and liberated very little heat when they decomposed.

Finally, a very persuasive argument against the minimum rearrangement concept is the structure of styphnic acid, a primary explosive.

OH
O_2N NO_2
OH
NO_2
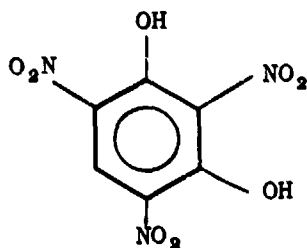
It is hard to see how that molecule can decompose without considerable atomic rearrangement.

3. Substituency Effects in Tetrazoles

The fulminates and tetrazoles are the only classes of compounds other than azides that have received systematic investigation of properties, the latter principally at the Explosives Research and Development

14

Establishment in Waltham Abbey. As listed in Table 1, a large number of
tetrazole salts and covalent structures have been synthesized and charac-
terized for usefulness as detonants. One, mercury 5-nitrotetrazole, has
also been investigated by the U.S. Navy and is now proposed as a replace-
ment for lead azide.[9]

Sufficient data on tetrazoles have been accumulated to allow
research workers to make a few structure/property correlations. Bates
and Jenkins[10] have suggested that the ranking in explosive behavior of
twelve 5-substituted nitrotetrazoles could be related to the substituent's
electron withdrawing power: the more electron withdrawing, the more
explosive the compound. The ranking observed for the substituent in
the 5 position ranged from mild ignitions for methyl 5-nitrotetrazole
to instability in the following order: $CH_3 = C_6H_5$ (mild ignitions),
$< NH_2 < H < NHNO_2$ (compounds explode), $<$ bis(tetrazole) $< 5,5'$-azo-
ditetrazole (do not detonate RDX), $< Cl < NO_2$ (very powerful explosives)
$< N_3$ (very sensitive) $< -N_2^+$ (unstable).

The salts of 5-nitrotetrazole could also be ranked according
to their sensitiveness. The salts of silver, mercury, and lead gave
more sensitive compositions and greater initiating power than the alkali
metal salts. The same salts of 5-chlorotetrazole were too sensitive
and corrosive, and those of 5-azidotetrazole were too hazardous.[11]

Haskins[12] has compared molecular orbital calculations of some
azide and tetrazoles with explosive behavior, dipole moments, and
binding energies. He used an iterative extended Huckel molecular
orbital approach to calculate dipole moments of 1-(H)tetrazole, 2-(H)tetra-
zole, and 5-aminotetrazole and found good agreement with experimental
measurements. For example, 1-(H)tetrazole was calculated as 5.269μ
and measured as 5.11μ. Binding energies calculated by the similar
extended extended Huckel molecular orbital (EHMO) method for the 1-(H)

15

and 2-(H) compounds were also in good agreement with experimental measurements.

Haskins also compared the empirical ranking of explosive behavior proposed by Jenkins with one devised according to total charge in the substituent group. Thus, EHMO results gave a quantitative measure of the electron withdrawing power of the substituents and gave an order: $CH_3 < H < NH_2 < NHNO_2 < N_3 < NO_2$. Haskins suggested that the EHMO calculations, although not in agreement with the qualitative ordering, were enough in agreement to indicate a relationship between explosive behavior and electron withdrawal power from the ring.

4. Physical Variables

The basic problem with structure-property correlations in primary explosives is the scarcity of quantitative data for a very large number of variables. From the structure standpoint alone, the number of candidate primaries within the families listed in Table 1 is very large, although they come within the classification generalities discussed earlier. Overlaying all chemical properties are the physical variables, which may determine whether a primary becomes a detonant. Physical variables of particle size and crystal form produce a wide variation in applicability to a detonator configuration; lead azide is a prominent example of physical variable influence. Even an explosive such as hexanitrostilbene (HNS), generally considered as secondary, can have primary sensitivity characteristics in superfine particle size, HNS I, in contrast to HNS form II which is relatively insensitive.[13] It appears that none of the sensitivity data can be used as a qualifying test for a primary.

However, we have proposed that one generally unmeasured property of primaries, deflagration to detonation transition (DDT), can be used for screening and classifying primary compounds. The property of fast

16

DDT (characteristic of lead azide), when combined with the observed characteristic that a primary will not extinguish when once ignited, may be a criterion for distinguishing primaries from secondaries, as a function of structure and independent of sensitivity properties.[*] The distinction at present is therefore one of degree; defining a primary in absolute terms is not possible with currently available information.

---

[*]Current practices contraindicate the use of DDT measurements as a necessary criterion; e.g., some primaries have long DDT lengths, such as lead styphnate.

17

III DEFLAGRATION TO DETONATION IN CAST EXPLOSIVES

A. Background

For DDT measurement to be a practicable screening procedure, a model system is needed to establish the basic approach. The objectives of the work reported here were to determine if such a measurement would permit one to relate the primariness of an experimental chemical structure, to a DDT result, in comparison with DDT test results of practical compounds such as the azides. Chemical structure relationships, primarily the effect of substituents, can be obtained by measuring a number of analog molecules of a class (as in the tetrazoles) or by measuring the effect of structural changes in isomers. The latter allows deductions to be made on compounds having the same empirical formula but differing in the position of a substituent.

A second requirement for this study was that the model compounds be castable since much DDT state of the art has been developed with cast secondaries. A survey of known "low melting" primaries revealed that both the 1- and 2-methyl derivatives of 5-nitrotetrazole fulfilled these requirements.

The research plan was based on the following assumptions:

(1) An important distinction between a primary and a secondary explosive is that a primary explosive undergoes very much faster deflagration-to-detonation transition (DDT).

(2) The difference between primaries and secondaries is one of degree rather than kind; therefore, experience obtained in measuring DDT in secondaries can be applied to primaries.

(3) It would be easier to develop a quantitative model for DDT in cast explosives.

18

The first assumption is based on the prime functions of primary and secondary explosives. Primaries are required to detonate rapidly when thermally ingited, whereas detonations in secondaries are initiated by shock waves. Possibly the faster the DDT, the better the primary although this premise requires a larger data base than is now available to support it. The inevitable DDT of a primary is also its weakness because accidental initiation of deflagration will result in detonation.

The second assumption is based on observations of the many similarities between primary and secondary explosives.[2b] Both primaries and secondaries will undergo DDT, although the transition takes longer and requires heavier confinement for secondaries. The existence of near primaries, such as some of the hydroxynitroaromatic compounds, and sensitive secondaries like PETN suggests that there may be many other compounds between the main body of primaries and the main body of secondaries that have received little attention because there is no obvious practical use for them.

The third assumption is based on the results of DDT research on secondary explosives. A first-generation model that gives order of magnitude agreement with experimentally determined times and distances for DDT in cast secondaries has been formulated by Macek.[14] No equivalent model of DDT in porous secondaries exists. The work of Bernecker and Price[15] indicates that the formation of a convective flame front over a large surface area and a resulting complex flow field preceed DDT in a porous explosive-based propellants, a clearer understanding of the role of convective burning in DDT in proous explosives may eventually be developed. At present, however, the basic physical processes involved in DDT have been determined only for cast explosives in which convective burning does not occur.

Many of the physical variables found in crystalline test compounds, such as density and crystal size and shape, were eliminated by using cast

primaries. The most important variable, chemical structure, was retained by studying two isomers, 1-methyl-5-nitrotetrazole (1-MNT) and 2-methyl-5-nitrotetrazole (2-MNT). These compounds were synthesized as described in Appendix A, and their heats of formation, detonation velocities, and Chapman-Jouguet pressures were calculated (see Appendix B).

The specific objectives were to measure the times to DDT for cast 1-MNT and 2-MNT and to develop and test a first-generation model of DDT in cast primaries that relied on experimental input data. To meet these objectives, the work was divided into the following five tasks.

Task 1: Measure the time-for-DDT on cast 1- and 2-methyl-5-nitrotetrazole (1-MNT and 2-MNT).

Task 2: Conduct well-instrumented hot-wire initiation experiments on 1-MNT and 2-MNT to measure the pressure-time histories in the deflagration regions and the times and distances for detonation.

Task 3: Analyze Macek's model for DDT in cast secondary explosives and apply it to DDT in cast primaries.

Task 4: Test this DDT model on the existing DDT data for single crystals of lead azide.

Task 5: Use the experimental pressure-time data obtained in Task 2 to predict the times and distances for DDT for 1-MNT and 2-MNT and compare the predictions with the experimental results.

B.   DDT Measurements on Cast 1-MNT and 2-MNT

The time for DDT was measured for cast 1-MNT and 2-MNT by using the technique developed by Leopold[16] and modified by Goodale.[3] The initiator plug and charge holder are shown in Figure 3. The bridgewires were 1-mil Nichrome wires soldered across the center of the charge holder. A plastic monofilament light pipe of 40 mils diameter was placed in the phenolic plug with its upper surface immediately under the bridgewire to determine the time of initiation of burning in the explosive by observing the first light emission near the bridgewire. A second light

20

LIGHT PIPE

ALUMINUM CHARGE HOLDER

REMOVABLE GUIDE

BRIDGE WIRE

EXPLOSIVE

INSULATING WASHER

PHENOLIC PLUG

LEADS TO
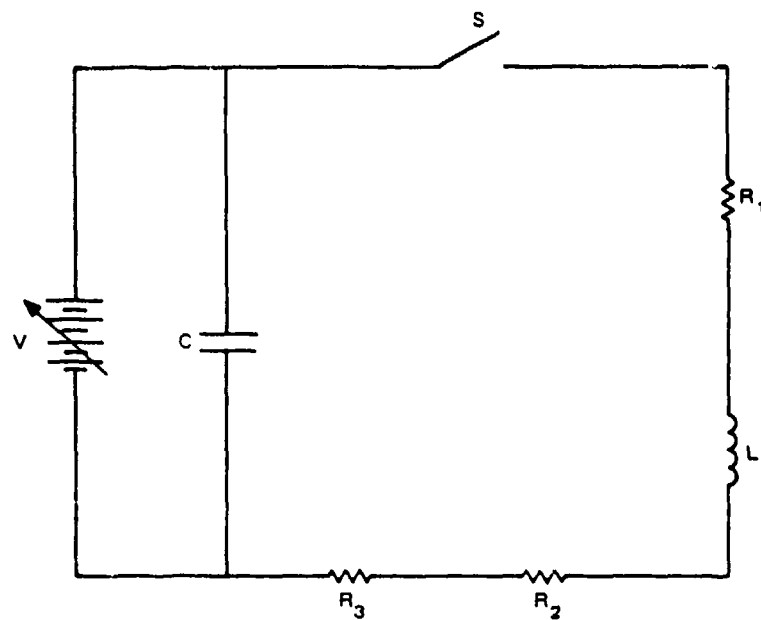BRIDGE WIRE

LIGHT PIPE
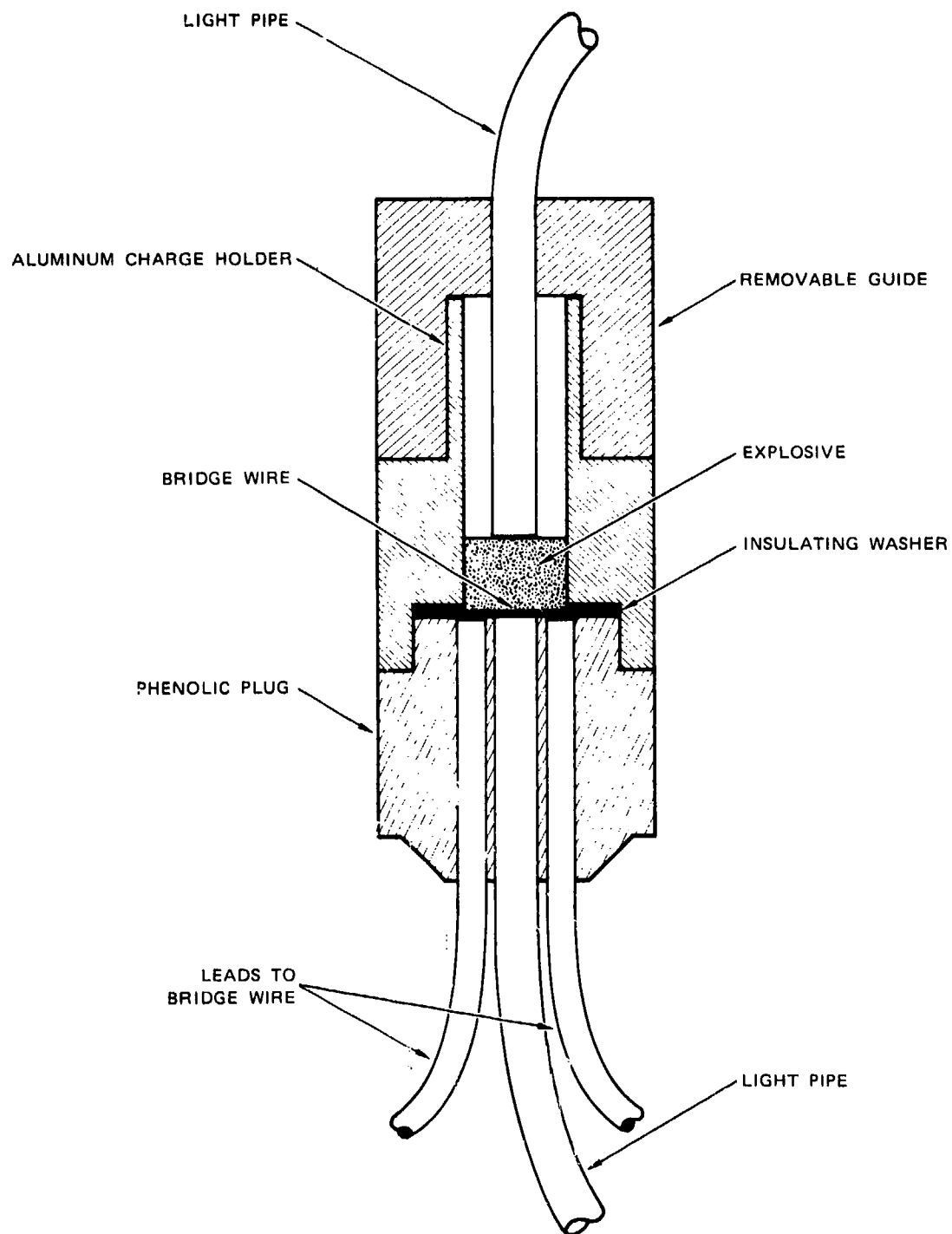
SA-3692-2

FIGURE 3   INITIATOR PLUG AND CHARGE HOLDER

21

pipe was inserted into the top of the charge holder and placed directly
on the upper surface of the cast explosive to detect the light emitted
by the detonation wave as it reached the top of the charge.

The capacity-discharge firing circuit diagrammed in Figure 4 was
used to ignite the explosive charges. The waveforms of the current
discharge through the bridgewire, as represented by the voltage drop
across a constant, noninductive resistance close to the bridgewire in
the circuit, was monitored in each test on an oscilloscope. Reproducible
current pulses free from anomalous irregularities required the use of a
vacuum switch of high current capacity. The resistance of each bridgewire
was measured before each test to ensure that the bridgewire connections
remained intact and that the resistance remained in the normal range
of 4.5 to 7.5 ohms.

The electronic recording system was slightly different from that
used previously.[3] As in the previous study,[2b] a dual-beam oscilloscope
was used to record the capacitor-discharge pulse and the light emitted
by the ignition of the explosive. A single-beam oscilloscope with a
very sensitive triggering mechanism was used to record the light output
observed by the lower light pipe. A pulse generator was added to the
circuit to produce a time reference peak at 0.6 μsec after the triggering
of the lower photomultiplier by the light emitted by the ignition of
the charge. To facilitate observation of the entire trace, the triggering
pulse was delayed for 1.57 μsec and then sent to the lower photomultiplier.
Another single-beam oscilloscope, also triggered by the ignition of the
explosive, was used to record the light output from the upper light pipe.

Accurately weighed 5-, 10-, 20-, and 40-mg charges of 1-MNT and
2-MNT were transferred into charge holders and pressed at 5000 psi.
These pressed charges were then melted to obtain cast, fully dense
charges. The initial castings of 2-MNT contained numerous voids and

C - Capacitor - 1.0 microfarad

S - Vacuum Switch

L - Circuit Inductance - 1 6 microhenries

R_1 - Circuit Resistance - 0.31 ohm

R_2 - Coaxial Current Shunt - 0.006 ohm

R_3 - Bridgewire - 4.5 to 7.5 ohms

SA-4770-1

FIGURE 4   FIRING CIRCUIT

rough surfaces because they were allowed to solidify too rapidly. A casting procedure was developed in which a slow cooling rate and continuous observation through a microscope were used to ensure reliable casting. The resulting cast 2-MNT charges had extremely flat upper surfaces and an average density of 1.672 g/cm^3. Considering the small weights (5-40 mg) and measured charge lengths (0.5-5 mm), this average density was in good agreement with the literature value[17] of 1.64 g/cm^3.

The same casting procedure was then used to prepare the cast 1-MNT charges. Because of its low melting point (58°C compared with 86°C for 2-MNT), 1-MNT cooled relatively slowly and exhibited a large degree of supercooling before solidifying into a glass. By using a faster cooling rate, fully dense, crystalline charges of 1-MNT were finally produced in the forms of microcrystals and relatively coarse crystals. All these forms of cast 1-MNT (glassy, microcrystalline, and coarse crystalline) were tested. The average density of the cast 1-MNT charges (1.775 g/cm^3) closely agreed with the value of 1.76 g/cm^3 predicted by a group additivity approach previously described.[2]

Since both cast 1-MNT and 2-MNT were found to be somewhat transparent to light, the tops of all charges were blackened with a thin film of India ink to prevent premature triggering of the upper photomultiplier by light transmitted from inside the reacting charge before the detonation wave reached the top surface of the charge.

To test the apparatus, we performed a series of time-for-DDT measurements on pressed lead azide charges prepared four years ago.[3] The mean time to DDT for these charges was 0.9μsec as compared with 0.7 μsec obtained previously. However, the range of deviations was similar to the range of deviations observed for freshly prepared lead azide. The slightly longer times to DDT may have been due to aging effects in the lead azide.

24

Two series of cast, 20-mg charges were fired at various capacitor charging voltages to determine the threshold voltages for initiation of 1-MNT and 2-MNT. For cast 2-MNT, the threshold voltage for 20-mg charges was approximately 100 volts, while discharges of 110 volts reliably detonated every 2-MNT charge fired. Therefore, capacitor charging voltages of 110 volts were used to make the quantitative measurements of time to DDT as a function of charge length for cast 2-MNT. Although it was expected that cast 1-MNT would have a similar threshold voltage, cast 1-MNT charges failed to explode at capacitor charging voltages of less than 375 volts, and only one-fourth of the charges exploded at that voltage. In most tests, sufficient pressure was generated to blow the charge holder off the plug. Usually unreacted 1-MNT remained in the charge holder, and no audible explosive effects were produced. At capacitor charging voltages above 200 volts, the light emitted by the glowing bridgewire was sufficient to trigger the sensitive lower photomultiplier before the explosive actually ignited. Thus the measured times to DDT for these high voltage tests were upper limits because they included the ignition delay time of cast 1-MNT.

To avoid this premature triggering at high voltages, a modified bridge-wire apparatus was fabricated in which the bridgewire was moved off center so that its glow would not be as readily sensed by the lower light pipe. This modified apparatus worked well at voltages below approximately 350 volts, but bridgewire glow remained a problem at the voltage required for cast 1-MNT initiation. Therefore, quantitative time to DDT versus charge length measurements could not be obtained for cast 1-MNT.

However, the large difference in threshold capacitor charging voltages for two cast isomers, 1-MNT and 2-MNT, is an important result because it indicates that chemical structure can play a major role in the performance of potential primaries. Because the threshold voltage of cast 2-MNT is approximately the same as that of pressed lead azide,[3]

25

cast 2-MNT, based solely on this test, appears to be a promising candidate primary explosive, while cast 1-MNT appears not to be a primary. At present the only tentative explanation of this behavior is that in 1-MNT the close proximity of the hydrogen atoms in the methyl groups to the oxygen atoms in the nitro group leads to sufficient hydrogen bonding and decreased sensitivity.
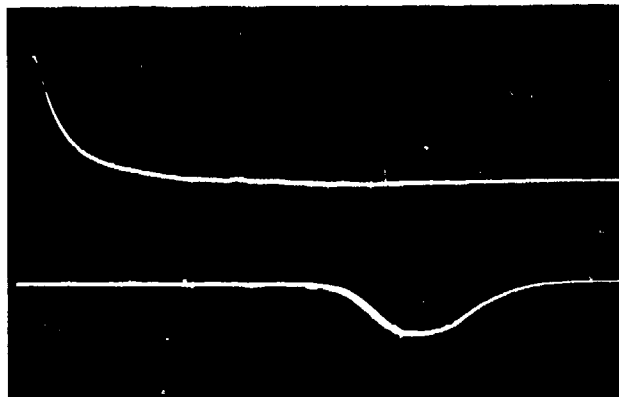
Quantitative data on time for DDT as a function of charge length were obtained for cast 2-MNT using a capacitor charging voltage of 110 volts. These cast charges varied in weight from 4 to 47 mg and in length from 0.4 to 5 mm. Charges weighing less than 5 mg failed to detonate, while approximately two-thirds of the 10-mg charges detonated. Charges exceeding 20 mg definitely detonated and damaged the aluminum charge holder to roughly the same extent as an equivalent mass of pressed lead azide. The experimental results for the fifteen cast 2-MNT charges that produced good oscilloscope records of three of these shots (shots 2M-45, 2M-34, and 2M-19 in Table 2) are reproduced as Figures 5, 6, and 7, respectively. Figures 5a, 6a, and 7a are the dual-beam oscilloscope records of the bridgewire current waveform and the light produced by the ignition of cast 2-MNT near the bridgewire. Practically all the energy from the capacitor discharge was deposited in the bridgewire in 4-6 μsec, and ignition occurred 11-16 μsec after the discharge began. The average time from the beginning of the energy pulse to the onset of burning for the cast 2-MNT charges listed in Table 2 was 13.7 μsec. The corresponding time to ignition for pressed lead azide at 105.9 volts was about 50 μsec.[3] Figures 5b, 6b, and 7b are the single-beam oscilloscope records of the light output detected by the lower photomultiplier after it had been triggered by the first light of ignition near the bridgewire. As previously mentioned, a reference pulse with a 0.6 μsec time delay and a time delay circuit of 1.57 μsec for the trace allowed observation of the entire lower photomultiplier output with a known time reference.

26

Table 2

SUMMARY OF TIME TO IGNITION AND TIME FOR DDT
EXPERIMENTS ON CAST 2-MNT

Charge Number	Capacitor Charging Voltage (volts)	Charge Length (mm)	Time to Ignition of Charge (μsec)	Time from Ignition to Detection of Light at Top of Charge (μsec)	Average Burning Rate (mm/μsec)
2M-16	110	0.488	12.8	4.4	0.111
2M-27	110	0.632	>20.0	2.6	0.243
2M-26	110	0.904	16.0	2.4	0.377
2M-24	110	1.214	19.0	4.0	0.3038
2M-10	110	1.621	12.4	2.0	0.8108
2M-14	110	1.717	12.5	2.0	0.859
2M-33	150	1.796	>10.0	3.6	0.499
2M-45	110	1.923	11.2	2.7	0.712
2M-35	110	1.991	13.1	3.2	0.622
2M-34	100	2.042	13.5	6.3	0.324
2M-46	110	2.223	12.2	1.9	1.11
2M-37	110	4.270	15.8	8.8	0.485
2M-19	110	4.425	11.8	8.6	0.514
2M-38[a]	135	4.493	----	7.5	0.599
2M-20	110	4.877	14.3	9.0	0.542

[a] After failing to ignite at 110 volts, Charge 2M-38 was ignited at 135 volts. No record of the capacitor discharge current pulse or the time to ignition was obtained.

27

a. BRIDGEWIRE CURRENT WAVEFORM

    Horizontal Scale: 2 μsec/cm
      Vertical Scale: 0.2 volts/cm

    PHOTOMULTIPLIER MONITORING
    LIGHT NEAR BRIDGEWIRE

    Horizontal Scale: 2 μsec/cm
      Vertical Scale: 0.2 volts/cm

b. LOWER PHOTOMULTIPLIER TRIGGERED
   BY FIRST LIGHT NEAR BRIDGEWIRE

    Horizontal Scale: 0.5 μsec/cm
      Vertical Scale: 0.2 volts/cm

    REFERENCE PEAK AT 0.6 μsec

    TIME DELAY OF 1.57 μsec

c. UPPER PHOTOMULTIPLIER TRIGGERED
   BY FIRST LIGHT NEAR BRIDGEWIRE

    Horizontal Scale: 1 μsec/cm
      Vertical Scale: 0.2 volts/cm

    REFERENCE PEAK AT 0.6 μsec

SA-4770-2

FIGURE 5   OSCILLOSCOPE RECORDS FOR SHOT 2M-45

a. BRIDGEWIRE CURRENT WAVEFORM

   Horizontal Scale: 2 μsec/cm
     Vertical Scale: 0.2 volts/cm

   PHOTOMULTIPLIER MONITORING
   LIGHT NEAR BRIDGEWIRE

   Horizontal Scale: 2 μsec/cm
     Vertical Scale: 0.2 volts/cm
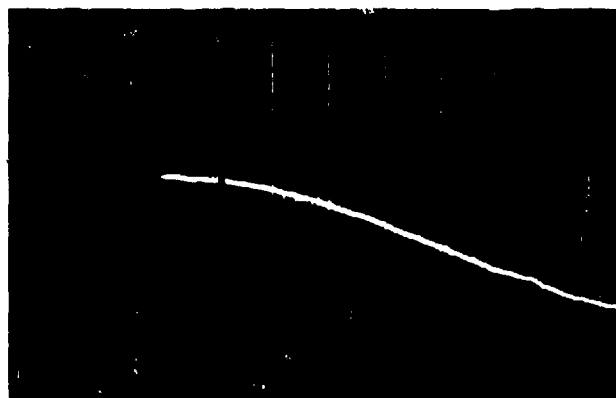
b. LOWER PHOTOMULTIPLIER TRIGGERED
   BY FIRST LIGHT NEAR BRIDGEWIRE

   Horizontal Scale: 0.5 μsec/cm
     Vertical Scale: 0.2 volts/cm

   REFERENCE PEAK AT 0.6 μsec

   TIME DELAY OF 1.57 μsec
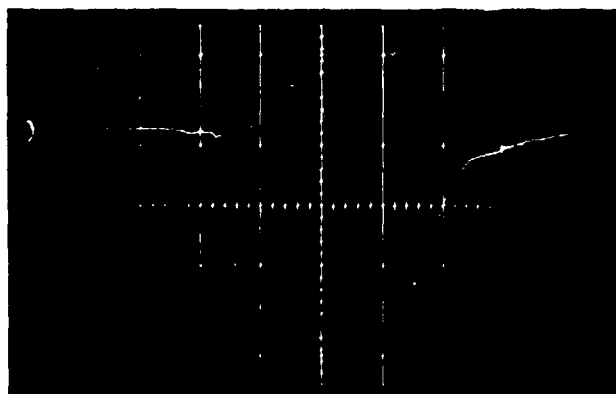
c. UPPER PHOTOMULTIPLIER TRIGGERED
   BY FIRST LIGHT NEAR BRIDGEWIRE

   Horizontal Scale: 2 μsec/cm
     Vertical Scale: 0.2 volts/cm

   REFERENCE PEAK AT 0.6 μsec

SA-4770-3

FIGURE 6   OSCILLOSCOPE RECORDS FOR SHOT 2M-34
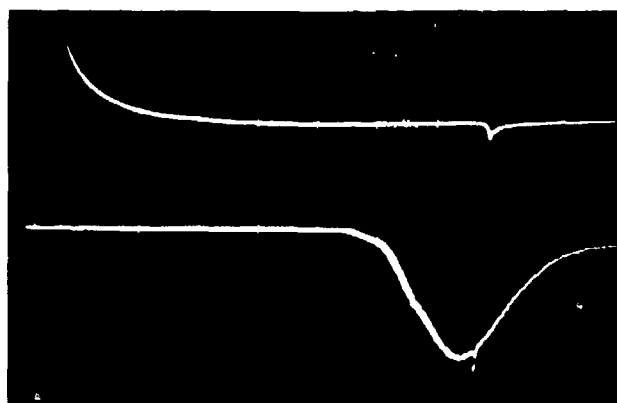
29
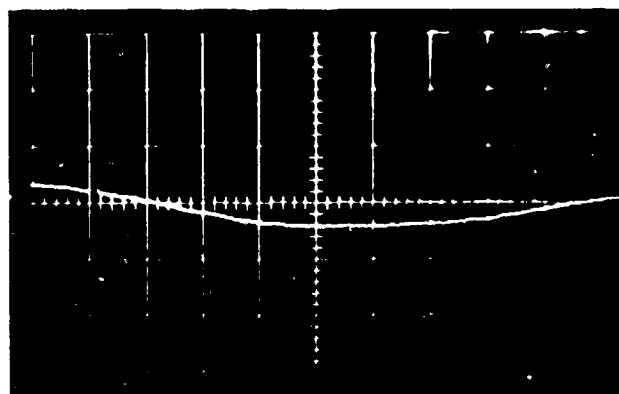
a. BRIDGEWIRE CURRENT WAVEFORM

    Horizontal Scale: 2 μsec/cm
      Vertical Scale: 0.2 volts/cm

    PHOTOMULTIPLIER MONITORING
    LIGHT NEAR BRIDGEWIRE

    Horizontal Scale: 2 μsec/cm
      Vertical Scale: 0.2 volts/cm

b. LOWER PHOTOMULTIPLIER TRIGGERED
BY FIRST LIGHT NEAR BRIDGEWIRE

    Horizontal Scale: 0.5 μsec/cm
      Vertical Scale: 0.2 volts/cm

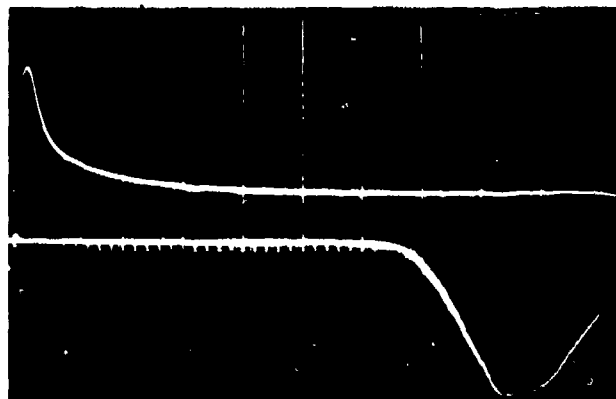   REFERENCE PEAK AT 0.6 μsec

    TIME DELAY OF 1.57 μsec

c. UPPER PHOTOMULTIPLIER TRIGGERED
BY FIRST LIGHT NEAR BRIDGEWIRE

    Horizontal Scale: 1 μsec/cm
      Vertical Scale: 0.2 volts/cm

    REFERENCE PEAK AT 0.6 μsec

SA-4770-4

FIGURE 7   OSCILLOSCOPE RECORDS FOR SHOT 2M-19
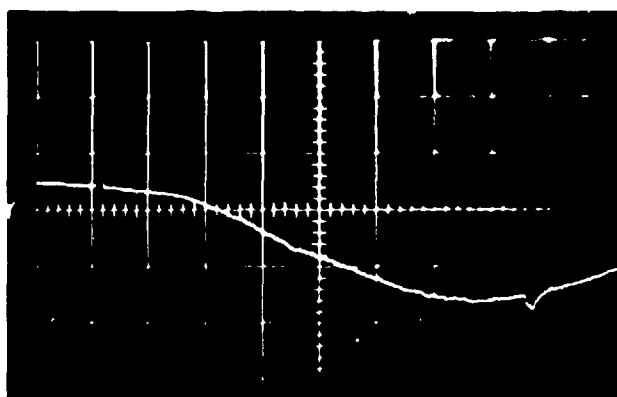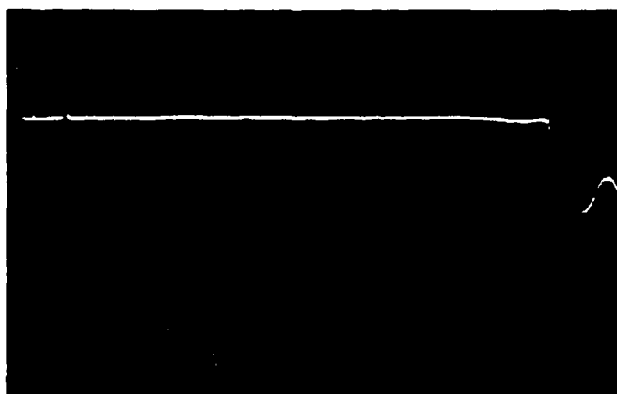
30

The duration of the light production at the bottom of the charge can be determined from records like Figures 5b, 6b, and 7b.

Figures 5c, 6c, and 7c represent the single-beam oscilloscope records of the light output detected by the upper photomultiplier after it had been triggered by the ignition of the charge. The 0.6-μsec reference peak also appeared on these records, which measured the time between ignition and the appearance of light at the top of the charge. This light was assumed to be caused by a detonation wave produced inside the charge that propagated through the remainder of the charge. The measured time was then taken as the time for DDT for that charge. The times for DDT in Figures 5c, 6c, and 7c are 2.7, 6.3, and 8.3 μsec, respectively. Because shots 2M-45 (Figure 5) and 2M-34 (Figure 6) were nearly the same charge length, the large difference in the times for DDT for these two shots indicated that the duration of burning before the onset of detonation in cast 2-MNT charges listed in Table 2 were found to be 4.60 and 2.68 μsec, respectively. These values are compared with previously determined values[3] for three other primaries in Table 3. All the primaries tested in this apparatus exhibited significant standard deviations in time for DDT. The absence of confinement on the upper surface of the explosive may result in upward movement of the charge during deflagration. This motion could contribute to the variation in burning times. Cast 2-MNT exhibits a much larger standard deviation in the times for DDT than the other three primaries. However, its mean time for DDT is less than that of lead styphnate and FDIPAM and, therefore, cast 2-MNT qualifies as a good primary based on relative DDT times.

If the course of DDT were exactly repeatable in successive experimental charges of varying lengths, a plot of charge length as abscissa against time between ignition at one end of the charge, and appearance of light at the other would appear as a single well defined curve. This curve would rise from the origin with an initially steep slope representing the

31

Table 3

TIME FOR DDT FOR CAST 2-MNT AND OTHER PRIMARY EXPLOSIVES

	Lead Azide	Lead Styphnate	FDIPAM	Cast 2-MNT
Number of charges fired	20	29	27	15
Capacitor voltages (volts)	105.9	67.8	131.2	110.0
Average charge length (mm)	1.43	1.94	2.74	2.31
Mean times from ignition to detection of light at the top of the charge (μsec)	0.65	11.20	9.81	4.60
Standard deviations of times from ignition to detection of light at the top of the charge (μsec)	0.115	1.110	1.660	2.68

initial slow propagation of the deflagration wave. The slope would decrease with time until it reached a constant value corresponding to the detonation velocity of the explosive. The time at which the detonation velocity was reached would be the time for DDT of the explosive.

The experimental times for DDT listed in Table 1 for cast 2-MNT are plotted as a function of charge length in Figure 6. The times for DDT vary greatly for charge lengths of less than 2 mm, while the times for DDT for 4-5 mm charges appear to be more consistent. The longer charge (Shot 2M - 38), which had a relatively short time for DDT (7.5 μsec), failed to ignite at 110 volts and was fired a second time at 135 volts. This double firing probably affected the performance of this shot. Omitting this result, a straight line with a slope of 3 mm/μsec is drawn in Figure 6 through the results for the remaining three longer charges. The detonation velocity of cast 2-MNT is considerably higher than 3 mm/ μsec (a TIGER code calculation[2b] resulted in a detonation velocity of 7.8 mm/μsec), but the scatter in the measured times for DDT prohibits an accurate determination of the detonation velocity. It is unrealistic to expect a good value of detonation velocity from these experiments on short charges because of the complex nature of DDT. To obtain useful detonation velocity data, the charges would have to be of sufficient length such that the time duration of the passage of the detonation wave is large compared with the time required for DDT.

In addition to the 3 mm/μsec line in Figure 6, we can draw another line with a much less steep slope through the shorter charge length results. A line with a slope of 0.1 mm/μsec is shown in Figure 6, although the large variation in times for DDT for these charges prohibits any quantitative conclusions. In fact, a line with a slope of 0.5 mm/μsec (the dashed line in Figure 6) can be drawn through all of the data. However, three observations indicate that the time-for-DDT behavior of cast 2-MNT is governed by a time-for-DDT versus charge-length relationship with an

33
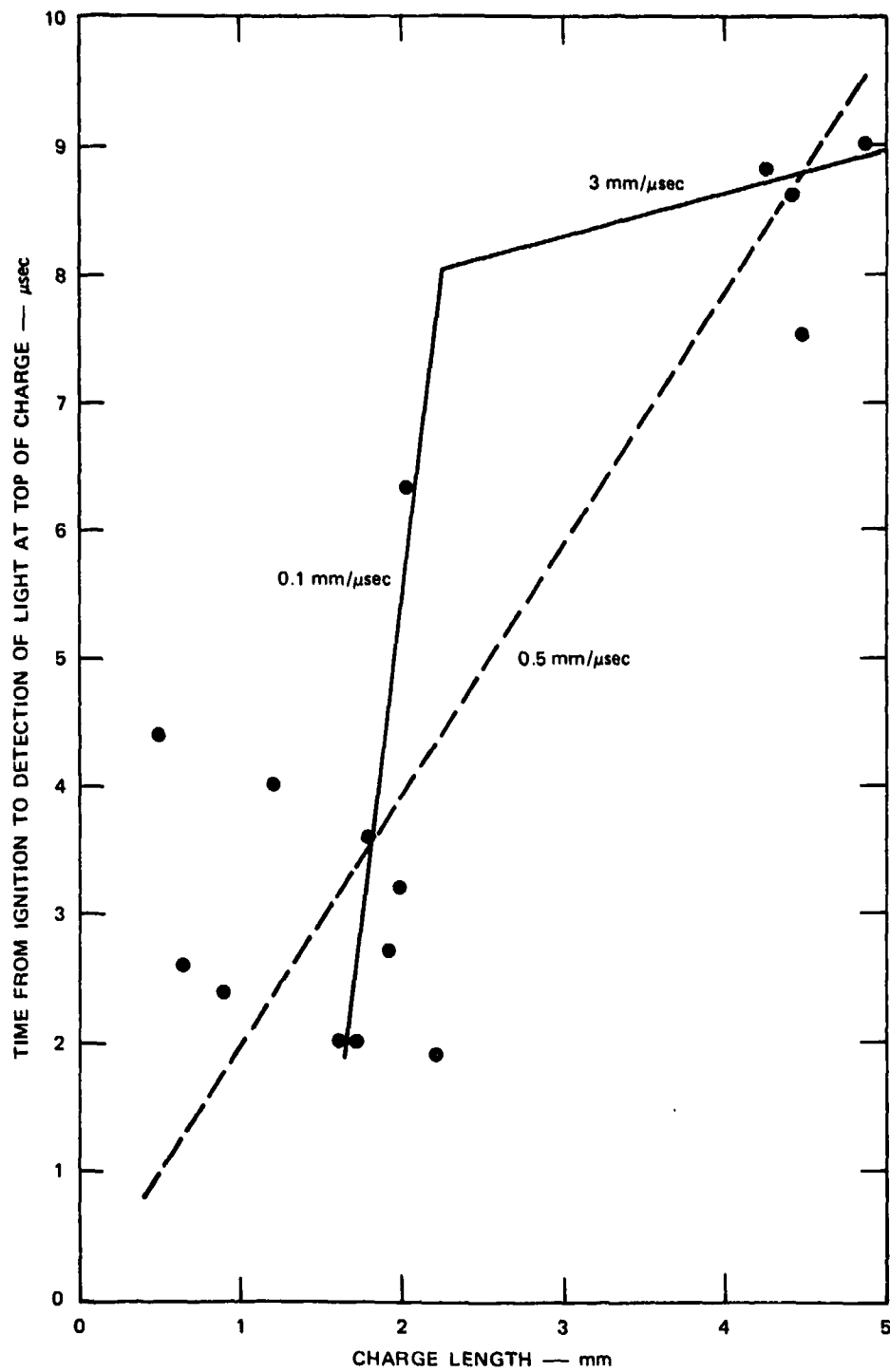
FIGURE 8   TIME TO DDT AS A FUNCTION OF CHARGE LENGTH FOR CAST 2-MNT

abrupt change in slope (such as the solid line in Figure 6). First, cast
2-MNT charges of approximately 1-mm length sometimes failed to detonate,
indicating that the critical length for full development of detonation is
more than 1 mm. Second, charges between 1.6 and 2 mm did show a trend
toward large increase in time for DDT over this small range of lengths.
Third, the three reliable sets of data for 4-5 mm charge lengths showed
the relatively small deviation (8.8 ± 0.2 μsec) typical of a fully devel-
oped detonation wave that had traveled some distance.

These three observations lead to the conclusion that the critical
charge length for DDT is approximately 2 mm in this experiment. This
critical distance agrees qualitatively with two results for lead azide.
In a thin flyer-plate impact study of shock-to-detonation transition (SDT)
in pressed lead azide, Davies et al.[18] found that the transition occurred
between 1 and 2 mm for shock waves that did not cause immediate detonation
at the explosive surface, but did cause buildup to detonation within the
explosive sample. Chaudhri and Field[9] concluded that single crystals of
lead azide less than 2 mm thick deflagrated rapidly but could not make the
transition to detonation that thicker crystals made. The determination
of this critical charge length is important to the design of the pressure
history experiments.

The main conclusions derived from the results of the time-for-DDT
experiments on cast 1-MNT and cast 2-MNT are:

(1) Cast 2-MNT is a much better candidate primary than cast
1-MNT because 2-MNT charges were readily initiated by a
capacitor charging voltage of 110 volts, whereas 1-MNT
charges were rarely initiated even at 375 volts.

(2) Cast 2-MNT is a good primary in its ignition and DDT
properties since its threshold voltage is close to that
of pressed lead azide, its time to ignition is less than
that of pressed lead azide, and the mean time required
for DDT is longer than that of the lead azide but shorter
than that of lead styphnate.

35

(3) The critical length for DDT in cast 2-MNT is approximately
     2 mm, and the critical time required for the full develop-
     ment of detonation in the DDT process is roughly 8 μsec.

C. Modification of Macek's Model for DDT in Cast Explosives

Early work[20,21] on the transition from deflagration (slow pressure-
dependent burning) to detonation led to the hypothesis that the sequence
of events in the transition can be divided into three parts: a rapid
pressure increase behind the burning front that sends compression waves
through the front and into the unreacted explosive, the coalescence of
these compression waves into a shock wave in the unreacted explosive
some distance ahead of the flame, and the shock init' ion of a detonation
wave in the unreacted explosive. This sequence explained the observations
of detonation waves in gaseous and condensed explosives that traveled
back toward the burning front from the point of initiation of detonation.
Macek[14,22-24] then developed a first-generation experimental and theoretical
approach to the study of DDT in cast secondary explosives. Because this
research program entails the study of DDT in cast primary explosives,
an analysis of Macek's approach and the extension of this approach to
cast primaries were undertaken. This section describes the analysis of
Macek's approach and the derivation of an improved approach; the next
section describes the application of the improved approach to lead azide.

Macek's approach to the study of DDT in cast secondaries was to
make experimental measurements of the pressure-time history in the
deflagration region and of the time and position where detonation first
appeared. The apparatus used by Macek is shown in Figure 9. A strain
gage positioned on the outside of the tube was used to measure the
pressure-time history in the deflagrating explosive near the bridgewire.
Ionization probes were located at regular intervals to record the passage
of the deflagration wave or compression waves in the unreacted explosive.
The measured pressure-time rise was of the form

36
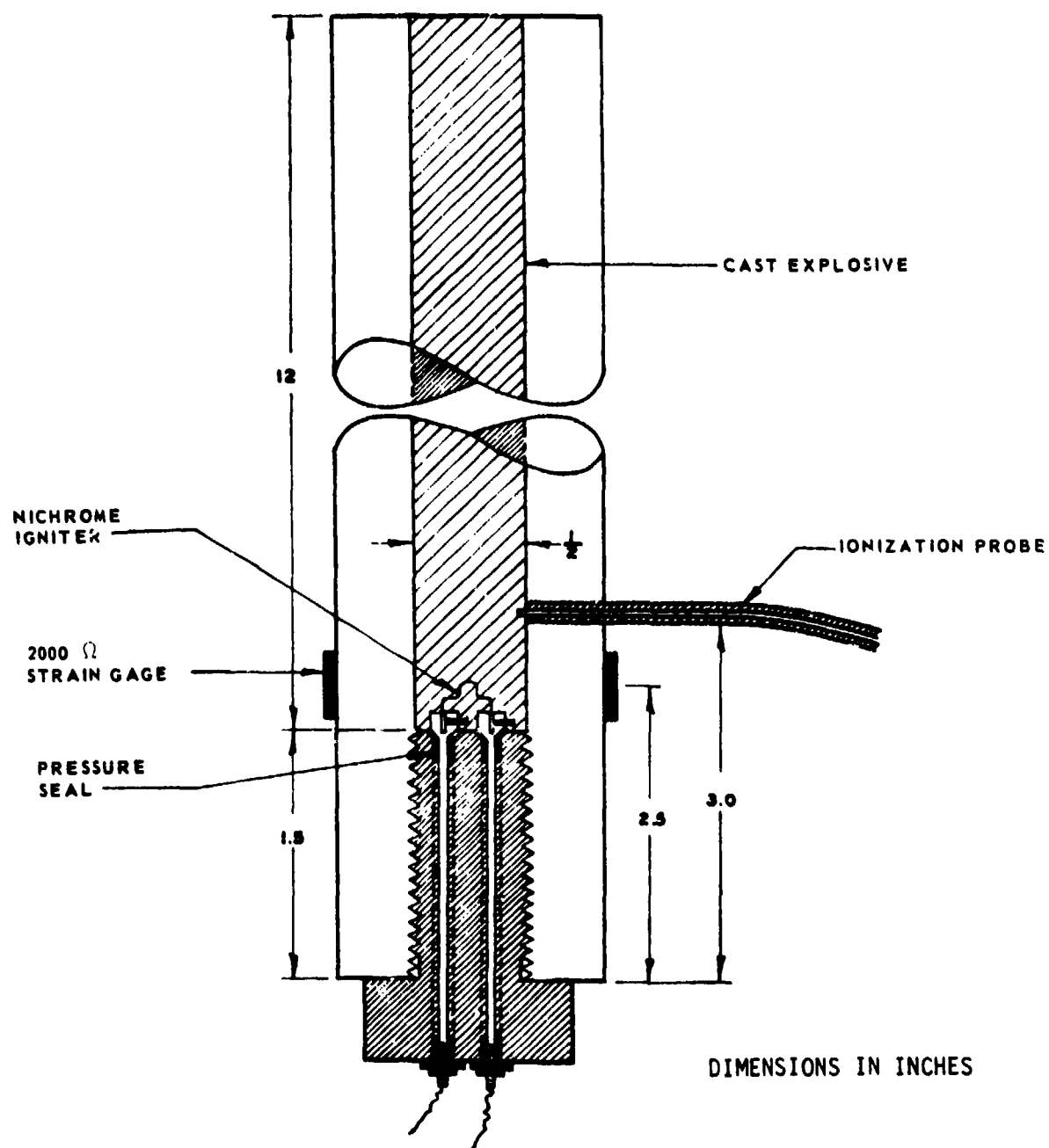
SA-4770-6

FIGURE 9 CHARGE ARRANGEMENT USED BY MACEK TO STUDY DEFLAGRATION
TO DETONATION TRANSITION

Three other ionization probes were located at regular intervals in addition to the
one shown.

$$P = P_o e^{kt} \tag{1}$$

where P_o is the initial pressure, t is the time, k is an experimentally determined constant, and P is the pressure in the reaction product gases. This pressure was assumed to be equal to the pressure in the unreacted solid explosive which obeyed the modified Tait compression equation

$$P = \frac{\rho_o c_o^2}{n} \left[\left(\frac{\rho}{\rho_o} \right)^n - 1 \right] \tag{2}$$

where ρ_o is the initial density, c_o is the initial sound velocity, ρ is the density of the compressed explosive, and n is a constant (generally $n = 3$). The propagation of the flame and its associated high-pressure gases into the solid explosive creates compression waves. The motion of these compression waves through the unreacted solid was calculated by the method of characteristics, which is illustrated in a distance-time diagram such as Figure 10. According to the Riemann analysis,[25] the quantity $u - \sigma$ is invariant along a negative characteristic $(u - c)$, where u is the particle velocity in the unreacted solid,

$$\sigma = \int \frac{c}{\rho} \, d\rho \tag{3}$$

and

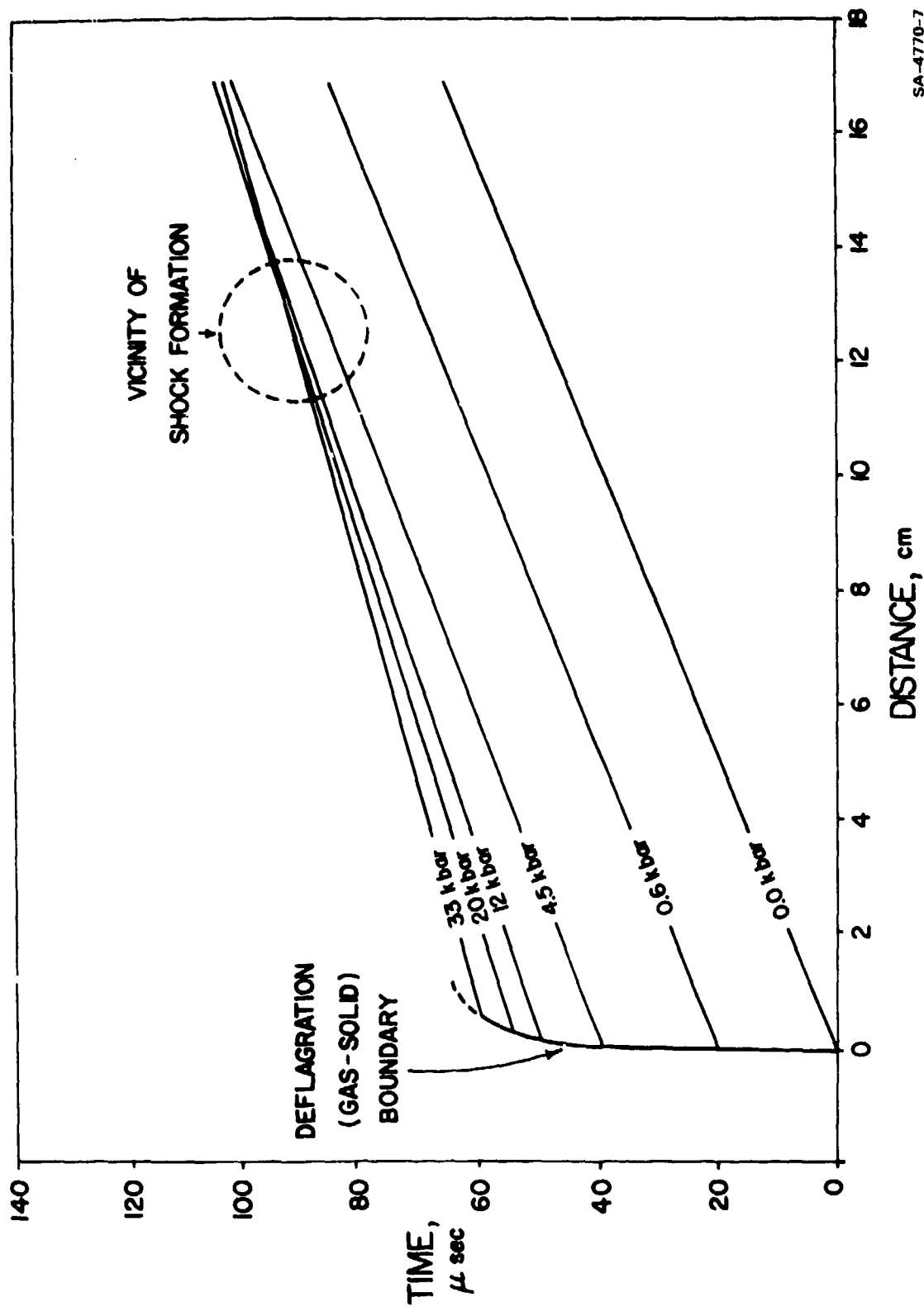$$c = \left(\frac{dP}{d\rho} \right)^{\frac{1}{2}} \tag{4}$$

For the modified Tait compression relation with $n = 3$,

$$c = \frac{c_o}{\rho_o} \rho \ (t) \tag{5}$$

and therefore

$$\sigma(t) = c(t) \tag{6}$$

38

FIGURE 10 CHARACTERISTICS DIAGRAM (C_+) FOR THE DEVELOPMENT OF A COMPRESSION WAVE FROM DEFLAGRATION IN A RIGIDLY CONFINED HIGH EXPLOSIVE

SA-4770-7

Thus, the characteristics in Macek's analysis were straight lines. As previously pointed out, straight-line characteristics assume that no reaction occurs in the compression region. Because the initial particle velocity was zero, the particle velocity was given by

$$u(t) = \sigma(t) - \sigma_o = c(t) - c_o \qquad (7)$$

The velocity of the compression waves was $u(t) + c(t)$ and the position $x(t)$ of the gas-solid boundary was

$$x(t) = \int_o^t (c - c_o)dt \qquad (8)$$

When the velocities of the compression waves were calculated at various pressures, and drawn in Figure 10 as C_+ characteristics $(u + c)$, the characteristics intersected at a distance of about 12 cm into the unreacted explosive. Figure 11 shows the development of the compression wave in pressure-distance plots at various times. This intersection of the characteristics was assumed to represent the formation of a shock wave of sufficient magnitude and duration to cause initiation of detonation in that region of the solid explosive. Once initiated, the detonation wave traveled through the unreacted explosive in the direction of flame propagation (detonation) and also toward the flame front (retonation).

Using this approach, Macek obtained qualitative agreement between calculated times and distances required for DDT and observed times ($\sim$ 100 μsec) and distances ($\sim$ 12 cm) for two cast secondaries, diethylnitramine dinitrate (DINA) and pentolite 50/50.[26] Macek also attempted to explain the observed exponential pressure-time relationship [equation (1)] behind the burning front on the basis of one-dimensional, adiabatic flame model. This flame had a burning-rate law of the form

$$R = \beta P^\lambda \qquad (9)$$

40
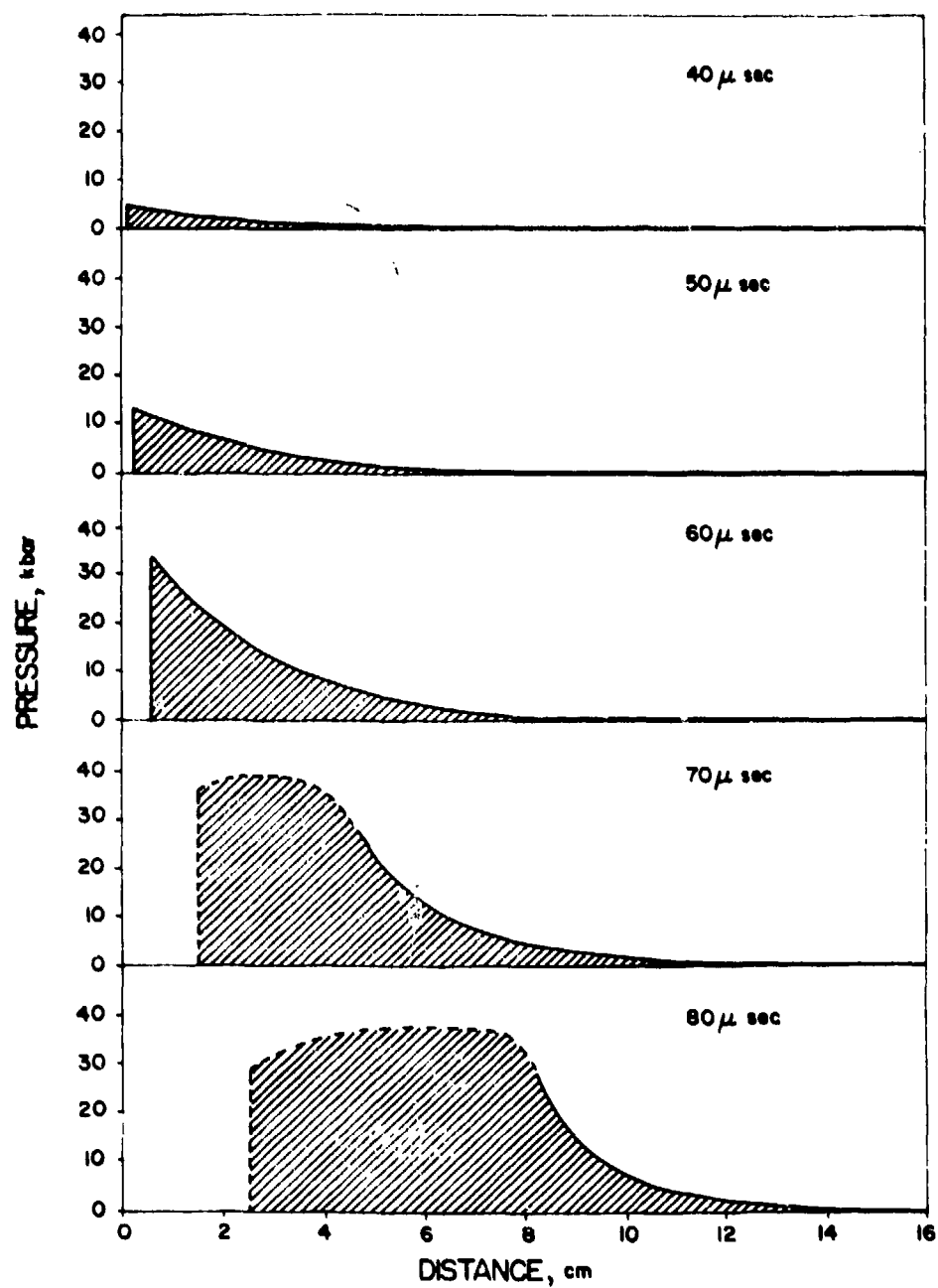
SA-4770-8

FIGURE 11 DEVELOPMENT OF COMPRESSION WAVE FROM DEFLAGRATION
AS TRANSPOSED FROM THE CHARACTERISTICS DIAGRAM
IN FIGURE 10

The left boundary of the shaded area represents the position of the
deflagration surface.

41

where R was the burning rate, β was a constant equal to 10 cm/sec-kbar, and λ was a constant equal to one. This type of burning-rate law has been observed for several explosives over a range of ambient pressures up to a kilobar by Andreev and Chuiko.[26] Macek normalized the pressure-time relationship derived for this burning-rate law to equation (1) through an adjustable proportionality constant that included the surface area of the burning front.

Although Macek's approach gave qualitative agreement with DDT experiments and contained many of the physical processes involved in DDT, it has several weak points that require modification. In the experimental setup, Macek used strain gages placed on the outside of the tube to measure pressure because those were the best available tools at that time. Recent advances in the use of in-material stress gages make these crude strain gage measurements obsolete. In particular, multiple Lagrange stress gages have been successfully used in reacting explosives[27] and near exploding bridgewires to measure detonator output.[28] The recommended use of these stress gages to measure pressure-time histories during DDT in cast 2-MNT is discussed in Section IV, Conclusions. In addition to better pressure measurements, the deflagration velocity measurements must be much more accurate than in Macek's model to determine the actual burning rate and surface area of burning as functions of time.

On the theoretical side of Macek's approach, three problems exist. By assuming that the pressures in the burned gases and in the unreacted explosives were equal, Macek neglected the pressure drop across a deflagration wave, which can be very large if the flame approaches a Chapman-Jouguet (CJ) deflagration. Thus the pressure in the unreacted explosive ahead of the flame may have been much higher than the pressures measured near the bridgewire in Macek's apparatus.

The second problem was pointed out by Jacobs,[29] who noticed that the linear pressure-burning rate relationship derived by Macek cannot describe

42

the pressure-particle velocity buildup at pressures above one kilobar.
He showed that Macek's linear pressure/burning rate relationship can
account for the exponential pressure/time relationship only when surface
area of the burning front is 20,000 times the original surface area of the
cast explosive. Even the introduction of mechanical means of increasing
the surface area available to the flame, such as fracture and induced
porosity, cannot account for that magnitude of surface area increase.
Therefore, the actual burning rate-pressure relationship in accelerating
deflagrations that cause detonation must be very different from the linear
burning rate-pressure law observed for explosives burning at high ambient
pressures and low ambient temperatures.[26]

The third problem with Macek's analysis is that the momentum imparted
to the burnt gases by the deflagration wave is neglected. In a closed
tube, this momentum participates in the flame acceleration mechanism.
Figure 12 shows the detonation and deflagration branches of the Hugoniot
curves in the pressure-volume and pressure-particle velocity planes. In
a detonation wave the pressure and particle velocity increase as the volume
decreases, while in a deflagration wave the pressure and particle velocity
decrease as the volume increases. When the deflagration wave is ignited
in a closed tube, it travels up the tube burning the explosive and creating
a flow of burnt gases in the opposite direction (i.e., toward the real wall).
As these gases contact the wall, their kinetic energy is converted into
internal energy. The resulting pressure increase interacts with the
deflagration wave, thereby establishing a mechanism of flame acceleration.
Because the accelerating deflagration wave is creating a compression field
in the unreacted explosive, a complicated nonsteady flow develops. This
flow consists of a compression field ahead of the flame in which particles
of unreacted explosive have a velocity in the forward direction and
accelerating turbulent flame zone in which the unreacted explosive burns,
loses its forward particle velocity, and becomes a burnt gas mixture with

43

(a) PRESSURE-VOLUME

(b) PRESSURE-PARTICLE VELOCITY
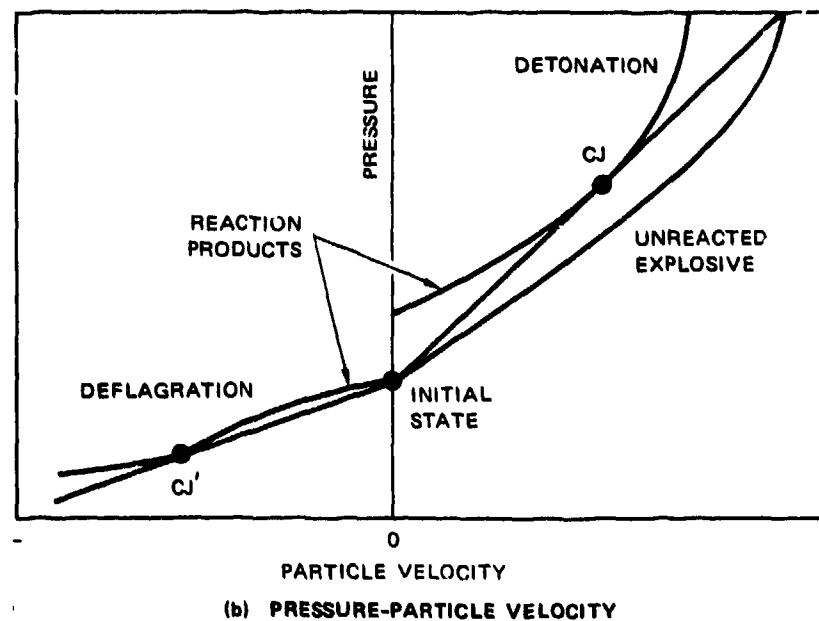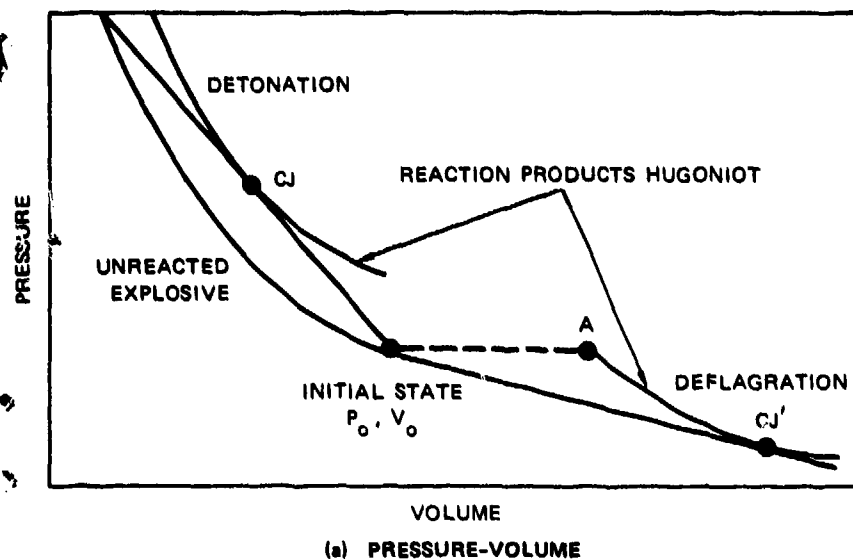
SA-4770-9

FIGURE 12   PRESSURE-VOLUME AND PRESSURE-PARTICLE VELOCITY DIAGRAMS
FOR DEFLAGRATION AND DETONATION

44

a negative particle velocity; and a compression zone behind the flame in which the burnt gases are slowed to the zero particle velocity rear boundary condition.

This complex flow is illustrated by a series of particle velocity-distance diagrams in Figure 13. This type of flow diagram for deflagration was first presented by Zeldovich and Kompaneets.[30] In Figure 13, the deflagration wave is shown as a discontinuity for simplicity but it actually has a finite width. In Figures 13a and 13b, the positive particle velocity of the compressed, unreacted explosive is less than the negative particle velocity imparted by deflagration, so a compression zone is required to bring the particle velocity to zero at the rear boundary. Figure 13c shows the unique case in which the particle velocity lost in deflagration exactly balances the particle velocity previously gained in compression. At later times, as illustrated in Figure 13d, the forward momentum is not totally destroyed by deflagration, and a rarefaction wave is created behind the flame to satisfy the rear boundary condition. However, once the compression zone behind the flame no longer exists, this flame acceleration mechanism also vanishes. The associated compression field preceding the flame must then be strong enough to shock initiate the unreacted explosive for DDT to occur.

Although an exact solution of the complex nonsteady flow field resulting from deflagration in a closed tube is extremely difficult, two analytical models of flame acceleration that provide upper and lower deflagration velocity limits have been formulated by considering the nature of the deflagration process. The pressure-volume diagram in Figure 12 shows that both the detonation and deflagration branches of the reaction products' Hugoniot curve have CJ states. For a detonation wave, the CJ state represents the only stable end state for the products,[31] but the end state of a deflagration wave may be represented by any point on the weak deflagration branch of the Hugoniot curve,[32] which is

45
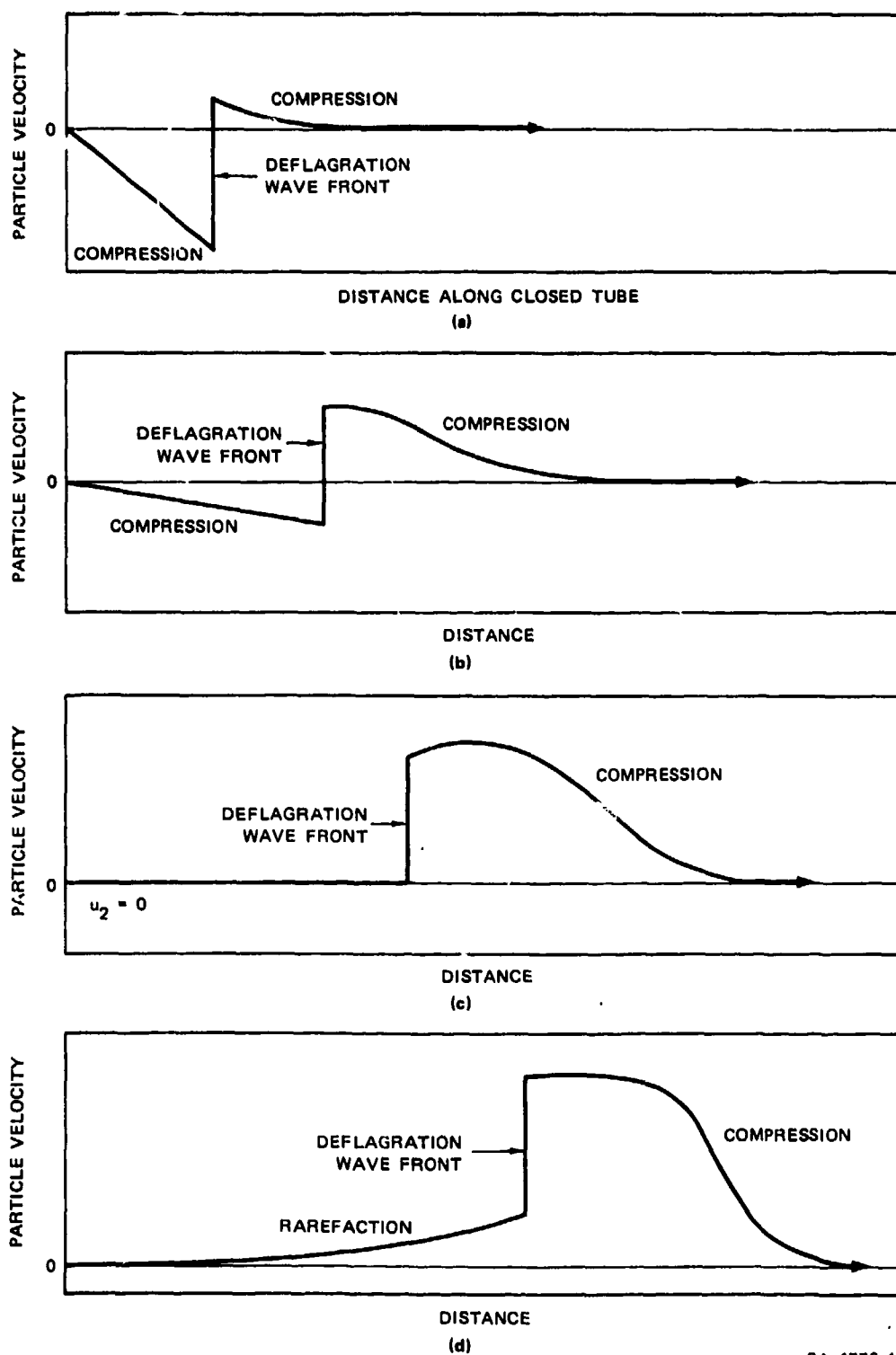
FIGURE 13   PARTICLE VELOCITY-DISTANCE DIAGRAMS FOR ACCELERATING
DEFLAGRATION WAVES

46

bounded by points A and CJ′ in Figure 13. Point A corresponds to a
constant pressure deflagration in which no particle velocity is produced
and point CJ′ corresponds to the maximum possible deflagration and particle
velocities and pressure drop. Thus the final state of a deflagration is
not well defined as it is in a detonation, but steady deflagration waves
in tubes tend toward the CJ state at long times.[32]

Combining the flame acceleration mechanism and the properties of
deflagration waves led to the formulation of two analytical models of
flame acceleration that bracket the actual deflagration process in a
closed tube. One model, originally used by Adams and Pack[33] for DDT
calculations in gases, consists of the compression region followed by
a deflagration wave whose velocity is always such that the forward
momentum imparted to the explosive by the compression waves is exactly
canceled out by the loss in forward momentum caused by deflagration.
The Adams and Pack model does not require a rarefaction or compression
wave to satisfy the rear boundary condition, and all of its states are
represented by Figure 13c. Since the change in particle velocity with
distance behind the flame is zero, the change in pressure at the rear
boundary with time must also be zero. Although this model conserves
momentum, it is not physically correct because it contains no flame
acceleration or rear wall pressure-time increase mechanisms. However,
the Adams and Pack model provides lower limits of the deflagration
velocity and pressure drop across an accelerating deflagration wave,
because any slightly faster deflagration produces negative particle
velocity and thus possesses the necessary mechanisms.

The second model of flame acceleration assumes that the deflagration
is always a CJ deflagration with the largest possible velocity and pressure
drop associated with a certain initial pressure. This model definitely
includes the flame-acceleration and rear-wall pressure-increase mechanisms
exhibiting all of the flow situations shown in Figure 13. The pressure-

47

particle velocity profiles for CJ deflagrations relating to Figure 13 are shown in Figure 14. This CJ deflagration model was discussed for DDT in gases by Troshin.[34] An interesting state where the two models predict the same velocity and burnt gas pressure is represented by Figures 13c and 14c. At this point the Adams and Pack deflagration becomes a CJ deflagration, and the CJ deflagration reaches a velocity for which the momentum loss during burning exactly cancels the forward momentum of the unreacted explosive.

For the CJ deflagration, this state also corresponds to the end of the flame acceleration mechanism of compression waves overtaking the deflagration wave. Table 4 shows the calculated properties of this state behind a shock wave in cast TNT and cast pentolite 50/50. The resulting shock pressures, 95 kbar for cast TNT and 129.5 kbar for cast pentolite 50/50, are too high to indicate a criterion for DDT, because pentolite, which readily undergoes DDT, has a shock sensitivity of about 20 kbar[35] and cast TNT, which does not undergo DDT, can be initiated by a 60-kbar shock.[27] Therefore, some other criterion for flame acceleration determines whether a cast explosive undergoes DDT.

These two analytical models of flame acceleration were used to make DDT calculations for cast pentolite, which is the only explosive for which a complete set of the required data was available. The method-of-characteristics part of Macek's analysis was used to predict the time and distance to shock formation ahead of the flame. The pressure-time histories used were those of Macek[14] up to one kilobar

$$P_2 = (0.08 \text{ kbar}) e^{0.12t} \tag{10}$$

and the more recent data of Price and Wehner[35] above one kilobar

$$P_2 = (1 \text{ kbar}) e^{0.08856(t-21.05)} \tag{11}$$
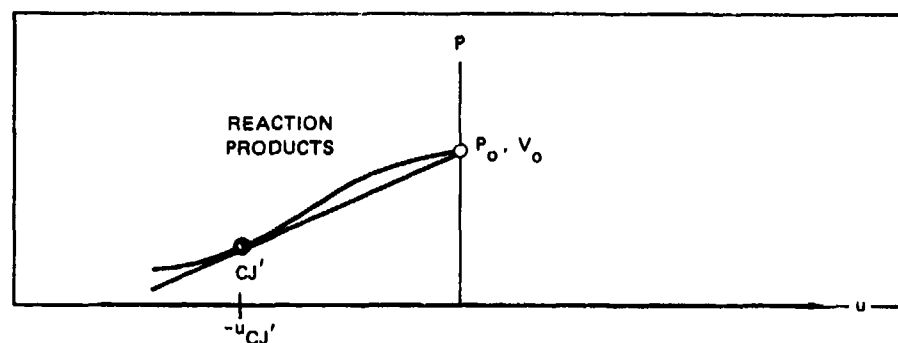
(a) CJ DEFLAGRATION AT INITIAL CONDITIONS P_o, V_o, $u_o = 0$
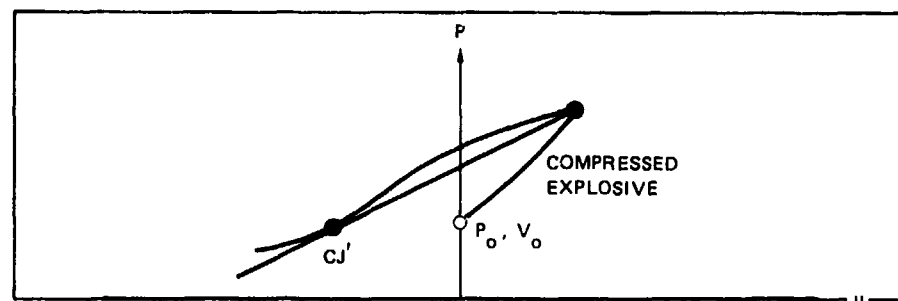
(b) CJ DEFLAGRATION IN SLIGHTLY COMPRESSED EXPLOSIVE
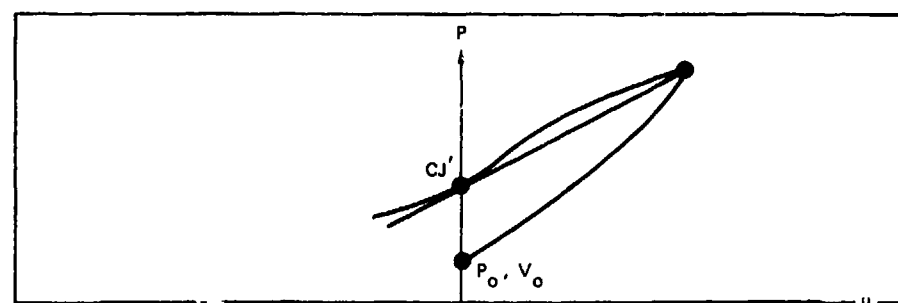
(c) CJ DEFLAGRATION TO A ZERO PARTICLE VELOCITY FINAL STATE
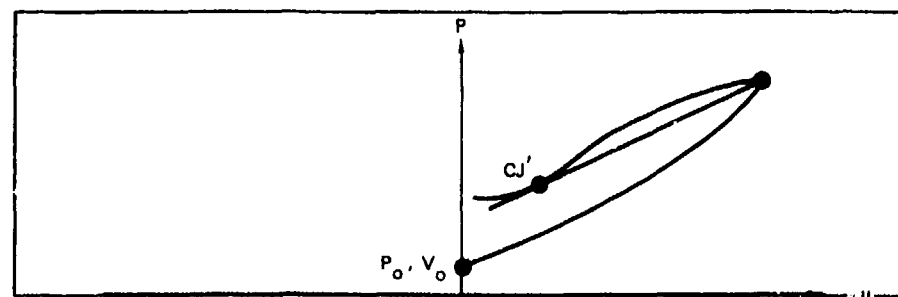
(d) CJ DEFLAGRATION TO A POSITIVE PARTICLE VELOCITY FINAL STATE

SA-4770-11

FIGURE 14   PRESSURE-PARTICLE VELOCITY PROFILES FOR CJ DEFLAGRATIONS
AT VARIOUS INITIAL PRESSURES

49

Table 4

CONDITIONS REQUIRED FOR A CJ DEFLAGRATION
TO A ZERO PARTICLE VELOCITY END STATE
BEHIND A SHOCK WAVE

	Cast TNT	Cast Pentolite 50/50
Shock Pressure in Explosive (kbar)	95.0	129.5
CJ Deflagration Velocity (mm/μsec)	3.116	3.504
CJ Pressure after Deflagration (kbar)	43.5	63.4

where P_2 is the pressure behind the deflagration and t is in microseconds.

The conditions ahead of the flame were determined by the equations for an isentropic compression with n = 3 in the modified Tait equation. The equations for the density ρ_1, particle velocity u_1, C_+ characteristics $(u_1 + c_1)$, and internal energy E_1 in terms of the pressure p_1 in the compressed unreacted explosive are

$$\rho_0 = \rho_1 \left(1 + \frac{3 P_1}{\rho_o c_o^2} \right)^{-1/3} \tag{12}$$

$$u_1 = c_o \left[\left(1 + \frac{3 P_1}{\rho_o c_o^2} \right)^{1/3} - 1 \right] \tag{13}$$

$$u_1 + c_1 = c_o \left[2 \left(1 + \frac{3 P_1}{\rho_o c_o^2} \right)^{1/3} - 1 \right] \tag{14}$$

$$E_1 - E_o = \frac{P_1}{2\rho_1} - \frac{c_o^2}{2} \left(1 - \frac{\rho_o}{\rho_1} \right) \tag{15}$$

The conservation equations across the deflagration wave are

$$\text{(MASS)} \quad \rho_1 (W - u_1) = \rho_2 (W - u_2) \tag{16}$$

$$\text{(MOMENTUM)} \quad P_1 + \rho_1 (W - u_1)^2 = P_2 + \rho_2 (W - u_2)^2 \tag{17}$$

$$\text{(ENERGY)} \quad E_1 + \frac{P_1}{\rho_1} + \frac{(W - u_1)^2}{2} + Q = E_2 + \frac{P_2}{\rho_2} + \frac{(W - u_2)^2}{2} \tag{18}$$

where the subscript 2 denotes the state behind the deflagration wave, W is the deflagration velocity and Q is the heat of reaction. The equation of state for reaction products is

51

$$P_2 \, \rho_2^{-K} = \text{constant} \tag{19}$$

and

$$E_2 + P_2/\rho_2 = \frac{K}{K-1} \, \frac{P_2}{\rho_2} \tag{20}$$

where K is the adiabatic expansion coefficient determined at the CJ detonation state through the equation

$$P_{CJ} = \frac{\rho_o D^2}{K+1} = 2 \, (K-1)Q \tag{21}$$

where D is the detonation velocity.

In the Adams and Pack model of zero particle velocity behind the deflagration, u_2 is set equal to zero and the resulting equation for the deflagration velocity in terms of state 1 is

$$W^2 + \frac{W}{u_1} \left[(K-1)(Q+E_1) - \frac{P_1}{\rho_1} + \frac{K-3}{2} u_1^2 \right] - (K-1)\left(Q+E_1 + \frac{P_1}{\rho_1} + \frac{u_1^2}{2} \right) = 0 \tag{22}$$

The pressure P_2 and density ρ_2 are then calculated from Equation (16) and (17) with $u_2 = 0$. Table 5 lists the input data on pentolite 50/50 required for the calculations and the calculated values of u_1, $u_1 + c_1$, W, and P_2 for various values of P_1, the pressure in the compressed, unreacted explosive. As shown in Table 5, the calculated deflagration velocities W are roughly 300 times faster than predicted by the linear pressure-burning rate relationship, Equation (9). Gibson and Macek[12] actually observed deflagration wave velocities of $10^5 - 2 \times 10^5$ cm/sec, so these calculated velocities appear to be of the correct magnitude. The closeness of the values for P_1 and P_2 clearly shows that the flame in the Adams and Pack model is a nearly constant pressure deflagration (corresponding to point A in Figure 11) for pressures below 20 kbar.

Table 5

INPUT DATA FOR PENTOLITE AND RESULTS
FOR DEFLAGRATION WAVES IN PENTOLITE (ADAMS AND PACK MODEL)

DATA ON PENTOLITE

Density = 1.67 g/cm^3

C_o = 2.43 x 10^5 cm/sec

D = 7.47 x 10^5 cm/sec

P_{CJ} = 259 kbar

K = 2.598

Q = 1.16 kcal/g

P_1 (kbar)	P_2 (kbar)	u_1 (cm/sec)	W(cm/sec)	$u_1 + c_1$ (cm/sec)
1	0.9998	2.440×10^3	2.489×10^3	2.479×10^5
2	1.9984	4.031×10^3	5.023×10^3	2.527×10^5
4	3.988	9.481×10^3	1.0228×10^4	2.620×10^5
7	6.937	1.6151×10^4	1.8358×10^4	2.753×10^5
10	9.815	2.249×10^4	2.700×10^4	2.880×10^5
20	18.75	4.171×10^4	5.700×10^4	3.264×10^5
30	26.36	5.864×10^4	8.860×10^4	3.603×10^5
40	32.56	7.385×10^4	1.201×10^5	3.907×10^5
70	44.47	1.1244×10^5	2.054×10^5	4.678×10^5
100	50.28	1.4410×10^5	2.738×10^5	5.311×10^5
123.8 (CJ state)	52.62	1.6597×10^5	3.186×10^5	5.749×10^5

The only other quantity required for a distance-time plot for DDT similar to that in Figure 8 for pentolite using this model is the position of the flame front as a function of time, $x(t)$, which is derived from

$$x(t) = \int_0^t W(t) \, dt \tag{23}$$

where $W(t)$ is determined from the dependence of W on P_2 in Table 4 and the dependence of P_2 on time from Equations (10) and (11). Figure 13 shows the resulting distance-time plot for pentolite using the Adams and Pack model of deflagration behind an isentropic compression. Comparing Figure 13 with Figure 8, the Adams and Pack model predicts a much more rapid deflagration and thus a greater penetration of the flame into the explosive. However, the time and distance required for shock formation are approximately the same in both diagrams.

These DDT predictions must also be compared with those for a CJ deflagration following an isentropic compression. At the CJ state, $W = u_2 + c_2$, or

$$(W - u_2)^2 = K \frac{P_2}{\rho_2} \tag{24}$$

Substituting Equation (24) into the conservation Equations (16) – (18) and solving for P_2 yields the following relationship

$$P_2 = (K-1) \, \rho_1 \, (Q + E_1) \left[1 - \sqrt{1 - \frac{(2Q + 2E_1 + P_1/\rho_1)P_1}{\rho_1 (K^2-1)(Q+E_1)^2}} \right] \tag{25}$$

and solving for ρ_2 gives

$$\rho_2^{-1} = \frac{(K-1)(Q+E_1 + P_1/\rho_1)}{KP_1} \left[1 + \sqrt{1 - \frac{K^2(2Q + 2E_1 + P_1/\rho_1)P_1}{\rho_1 (K^2-1)(Q+E_1 + P_1/\rho_1)^2}} \right] \tag{26}$$
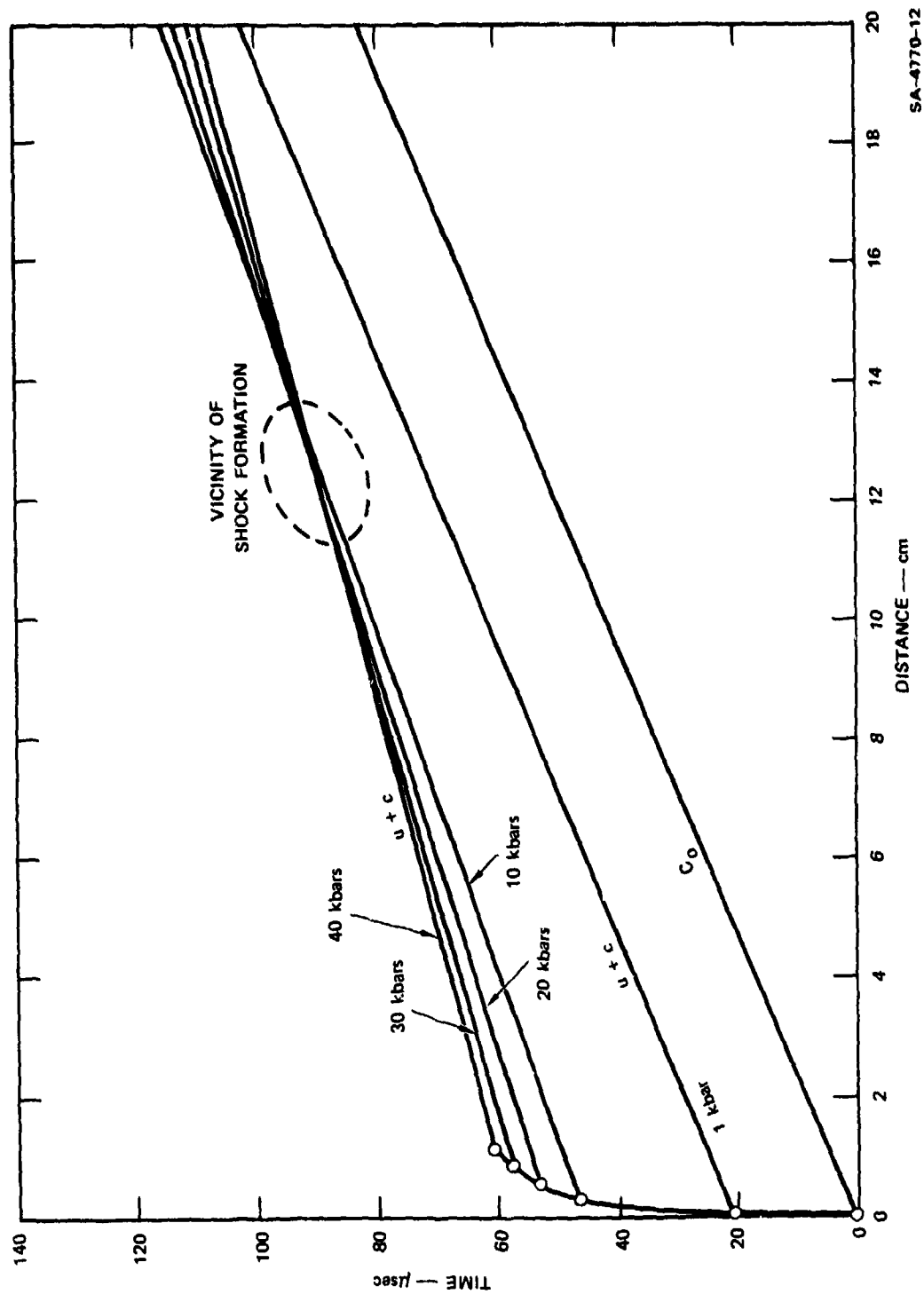
FIGURE 15 DISTANCE-TIME DIAGRAM FOR SHOCK FORMATION IN CAST PENTOLITE 50/50 USING THE ADAMS AND PACK MODEL OF DEFLAGRATION

The particle velocity u_2 behind the deflagration and the deflagration velocity W are then calculated from

$$W - u_2 = (KP_2/\rho_2)^{\frac{1}{2}} \tag{27}$$

and

$$W - u_1 = (W - u_2) \frac{\rho_2}{\rho_1} = \left(\frac{KP_2}{\rho_2}\right)^{\frac{1}{2}} \frac{\rho_2}{\rho_1} \tag{28}$$

Table 6 lists the calculated states for a CJ deflagration in isentropically compressed pentolite at various pressures. Figure 16 is the distance-time plot for DDT for the CJ deflagration model. The pressures P_2 behind the CJ deflagration wave are much lower than the corresponding values for the Adams and Pack model at low initial pressures P_1, and the CJ deflagration velocities are nearly twice as large as those in Table 5. In terms of the time and distance to DDT, the CJ deflagration front moves a greater distance into the explosive, and the shock formation occurs in a shorter time (about 80 μsec in Figure 16 compared with 90 μsec in Figure 15), whereas the distance to shock formation increases (about 14 cm in Figure 16 compared with about 13 cm in Figure 15).

Since these two analytical models represent upper and lower limits to the deflagration rate, the critical time and distance for DDT in cast pentolite 50/50 should be bracketed by these results if the isentropic compression of cast pentolite 50/50 obeys equation (2) with n = 3. More fully instrumented DDT experiments on pentolite are required to test the validity of these results but the distance, times, pressures, and velocities to be measured are defined by the following results:

(1) Rear wall pressure history measurements of 20-40 kbar in the first 50 μsec after ignition.

(2) Deflagration velocities of 10^4-10^5 cm/sec in the first 2 cm of explosive.

56

Table 6

CJ DEFLAGRATION WAVE CALCULATIONS
FOR ISENTROPICALLY COMPRESSED PENTOLITE

P_1 (kbar)	P_2 (kbar)	u_2 (cm/sec)	W(cm/sec)
1	0.2799	-2.044×10^5	4.500×10^3
2	0.5637	-2.019×10^5	8.910×10^3
4	1.1426	-1.958×10^5	1.7503×10^4
7	2.038	-1.870×10^5	2.986×10^4
10	2.966	-1.782×10^5	4.170×10^4
20	6.261	-1.5353×10^5	7.767×10^4
30	9.835	-1.3208×10^5	1.0962×10^5
40	13.65	-1.1304×10^5	1.3862×10^5
70	26.32	-6.539×10^4	2.130×10^5
100	38.54	-2.247×10^4	2.719×10^5
123.8	52.62	0	3.186×10^5

57
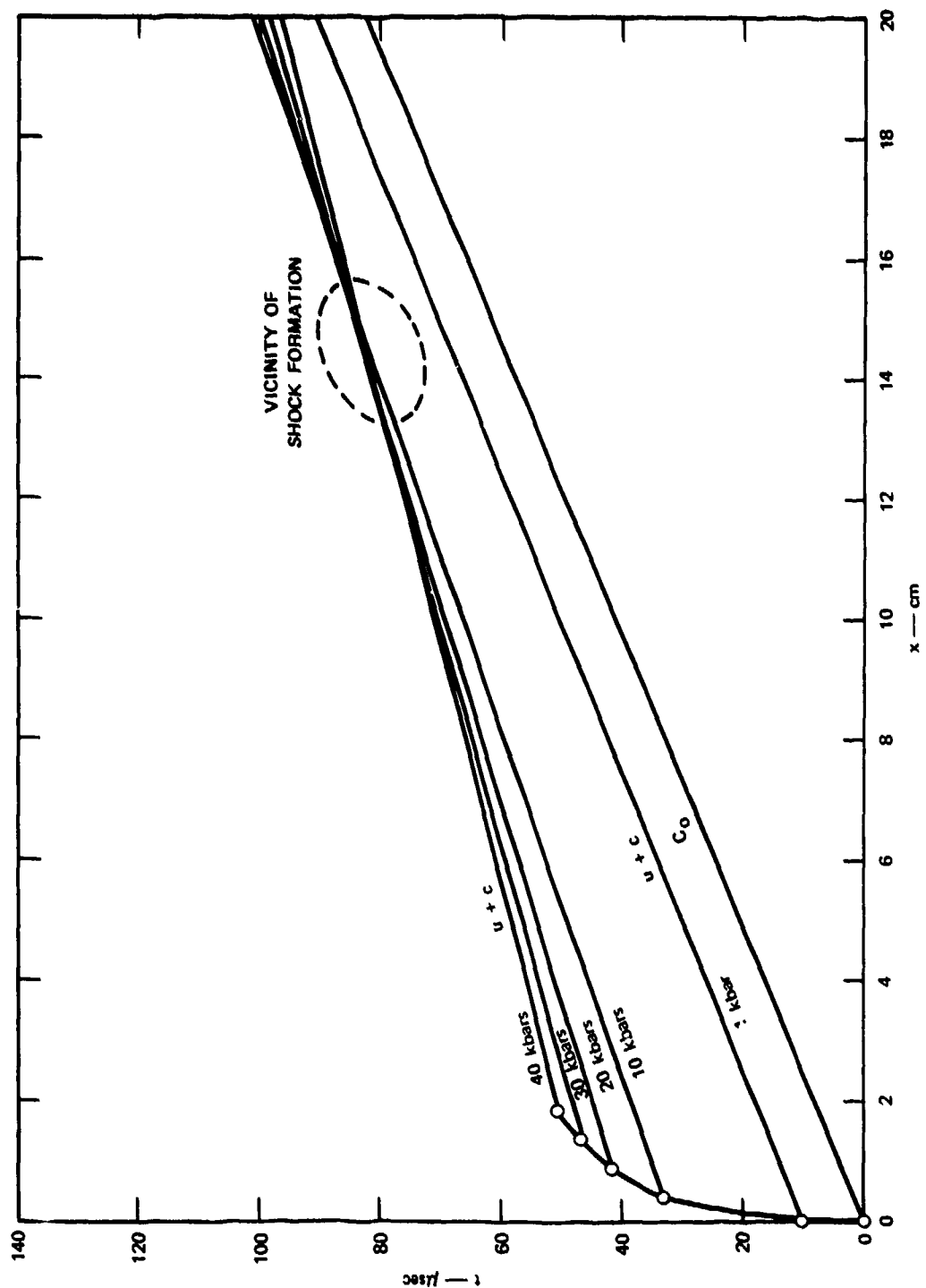
FIGURE 16   DISTANCE-TIME DIAGRAM FOR SHOCK FORMATION IN CAST PENTOLITE 50/50 AHEAD OF A CJ DEFLAGRATION WAVE

(3) Shock formation measurements at 13-14 cm into the
     explosive at times of 80-90 μsec after ignition.

DDT calculations using the Adams and Pack and CJ deflagration models
in the Macek approach yield much more realistic results than the original
burning rate model. In the next section, these models are used to make
DDT calculations on lead azide, the only primary for which some meager
data exist.

D. DDT and STD Calculations for Lead Azide

The processes of SDT[18] and DDT[19] have been quantitatively studied to
a limited extent in lead azide. Chaudhri and Field[19] observed very fast
deflagration waves in hot-wire initiation tests on lead azide crystals
of thicknesses below the critical thickness for DDT. By photographing
the deflagrating crystals under water, they measured the velocities and
pressures of the shock waves produced in the surrounding water by the
rapid deflagration of lead azide. These pressure data, combined with
Chaudhri and Field's framing camera records of the ignition process,
provide a rough estimate of the pressure-time history in the deflagration
region. Chaudhri's measurements[36] of the sound velocity and shock initia-
tion of lead azide crystals and Davies' measurements[18] of the unreacted
Hugoniot and sound velocity in lead azide pressed to a density of
3.4 g/cm^3 provided data on the properties of lead azide in the compression
zone ahead of the deflagration wave. Using these data in the two models
of deflagration discussed in the previous section, we calculated the
times and distances for DDT in lead azide crystals and pressed lead
azide and for SDT in pressed azide and compared them with the available
experimental results as a preliminary test of the DDT models.

To calculate the time and distance required for DDT in lead azide
crystals, we first related the pressure data obtained by Chaudhri and
Field[19] to the time after ignition. The actual pressures measured were

59

those of the shock waves produced in water as the lead azide deflagration front reached the end of the crystal. Using the acoustic approximation developed by Deal[37] for a detonation wave propagating into an inert material, the pressure in the lead azide, P_{LA}, is given by

$$P_{LA} = P_W \left(0.5 + \frac{\rho_{LA} U_{LA}}{\rho_W U_W} \right) \tag{29}$$

where P_W is the measured water pressure, ρ_W is the density of the water, U_W is the measured shock velocity in the water, ρ_{LA} is the density of α-lead azide crystals (4.60 g/cm^3), and U_{LA} is the measured velocity of propagation of the reaction front in the lead azide. Table 7 lists the measured values and the calculated pressures in the lead azide crystals. Since P_{LA} is the pressure at the front of the wave, it corresponds to P_1, the pressure in the unreacted explosive. These pressures were related to the time after ignition by examination of Chaudhri and Field's framing camera records of these reactions. In these records the framing rate was 0.7 μsec between frames and the transition from ignition to full development of the steady deflagration velocity for a certain crystal thickness took less than one frame. Thus the calculated pressures P_{LA} were assumed to be attained in less then 0.7 μsec. The largest pressure P_{LA} (12.85 kbar) was assumed to be de eloped in exactly 0.7 μsec and the c r two pressures were assumed to occur at times of 0.7 μsec minus the difference in crystal thicknesses divided by the average deflagration velocity (2.7 mm/μsec) in these experiments. The resulting pressure-time curve was of the form

$$P_{LA} = P_1 = (0.1 \text{ kbar})e^{6.94t} \tag{30}$$

where t is in microseconds.

The particle velocity u_1 in the unreacted lead azide was related to P_1 using the relationship

60

$$P_1 = \rho_o c_o u_1 \qquad\qquad (31)$$

which was found by Davies et al.[18] to hold for pressed lead azide at
pressures below 10 kbar. Chaudhri[19] reported a propagation rate for a
low amplitude longitudinal stress wave in lead azide crystals of
2.15 ± 0.3 mm/μsec. This value was taken for c_o in these calculations.
Actually, if the sound velocity is 2.15 mm/μsec, the waves that Chaudhri
and Field[19] refer to as fast deflagration waves are supersonic and therefore
are some sort of low-velocity detonation waves (LVD) that cannot develop
into high-velocity detonation (HVD) because of rapid pressure decay at
the edges of the crystal. A phenomenon like LVD has been observed for
lead azide pressed to high densities (3.75 g/cm^3) by Leopold.[38]

The remaining features of the DDT calculations are identical to those
described in the last section. Table 8 lists the input data for crystalline
lead azide and the results of calculations at various initial pressures
for the two deflagration models, the Adams and Pack model and the CJ
deflagration model. The calculated deflagration velocities for both
models are an order of magnitude lower than those observed by Chaudhri
and Field, while the velocities of C_+ characteristics ($u_1 + c_1$) are of
that magnitude ($\sim 2.5 \times 10^5$ cm/sec). Figures 17 and 18 show the distance-
time diagrams for DDT in α-lead crystals predicted by the Adams and Pack
and the CJ deflagration models, respectively. The calculated distances
for DDT are approximately 2 mm. This agrees with the observed behavior
of lead azide crystals of varying thickness. Crystals less than 2 mm
thick cannot undergo the DDT that thicker crystals readily make. The
calculated times to DDT are approximately 2 μsec and thus agree with
the preliminary results of Slagg,[39] who has measured times for DDT of
3 ± 2 μsec for crystals of lead azide.

The DDT calculations for crystalline lead azide exhibit order-of-
magnitude agreement with the experimental results and this is all that

61

Table 7

PRESSURES AND WAVE VELOCITIES FROM CHAUDHRI AND FIELD'S EXPERIMENTS ON α-LEAD AZIDE CRYSTALS

Crystal Thickness (μm)	Lead Azide Deflagration Velocity (mm/μsec)	Water Shock Velocity (mm/μsec)	Water Shock Pressure (kbar)	Calculated Lead Azide Pressure (kbar)
310	2.50	1.67	1.3	5.14
560	2.90	1.72	2.0	8.76
670	2.62	1.90	3.5	12.85

can be expected at the present time. The exact nature of the rapid deflagration or LVD waves in lead azide crystals is unknown. The framing camera records of the process indicate that some reaction occurs at the front of the wave. The general approach to DDT appears to be correct but the effect of reaction on the characteristics used in the shock formation part of the model needs to be considered.

The recent SDT experiments on pressed lead azide by Davies et al.[18] pioneered the use of stress gages in thin flyer plate impacts of primary explosives and also yielded data on the unreacted Hugoniot and on the time and distance for SDT. For lead azide pressed to a density of 3.4 g/cm^3, Davies found that stress waves propagate at 1.23 mm/μsec, and the equation for the Hugoniot curve in this case is obtained as

$$p_1 = 41.8 \ u_1 \qquad (32)$$

by substituting these values of c_o and ρ_o into equation 31. For both long pulses (3.5 μsec) and short pulses (0.1 μsec), in the 6-9 kbar range, Davies observed that the transition to detonation took about 2 μsec and occurred about 1-2 mm into the sample of pressed lead azide. To determine whether the theoretical approach to DDT developed in this report would predict similar times and distances, we used this unreacted Hugoniot for pressed lead azide and the pressure-time relationship of equation (30) in the CJ deflagration model to calculate the distance-time diagram shown in Figure 19. This calculation predicts a shorter time (1.2 μsec) and distance (0.9 mm) for pressed lead azide than for crystalline lead azide. This is mainly due to the lower sound velocity in pressed lead azide, which allows the compression waves to overtake each other more quickly. To compare a prediction of the CJ deflagration model to Davies' results, the SDT calculation shown in Figure 20 was made for an 8-kbar shock that causes the deflagration to begin about 0.6 μsec later in agreement with equation (30). This

63

Table 8

INPUT DATA FOR α-LEAD AZIDE CRYSTALS AND DEFLAGRATION VELOCITY CALCULATIONS

DATA ON α-LEAD AZIDE

ρ_o = 4.60 g/cm^3 Q = 115 kcal/m = 1.652 × 10^{10} erg/g K = 3.199 c_o = 2.15 mm/μsec

DDT Calculations

P_1 (kbar)	u_1 (cm/sec)	$u_1 + c_1$ (cm/sec)	Adams and Pack Model ($u_2 = 0$)		CJ Deflagration Model	
			P_2 (kbar)	W(cm/sec)	P_2 (kbar)	W(cm/sec)
5.14	5197	2.252 × 10^5	5.127	5.711 × 10^3	1.269	1.154 × 10^4
8.76	8857	2.324 × 10^5	8.698	1.032 × 10^4	2.214	1.943 × 10^4
12.85	1.299 × 10^4	2.403 × 10^5	12.65	1.608 × 10^4	3.325	2.813 × 10^4
25.78	2.607 × 10^4	2.644 × 10^5	24.31	3.712 × 10^4	7.080	5.338 × 10^4
101.7	1.0283 × 10^5	---	38.68	2.019 × 10^5	(CJ + u_2 = 0 models coincide)	

FIGURE 17   DISTANCE-TIME DIAGRAM FOR DDT IN α-LEAD AZIDE CRYSTALS USING ADAMS AND PACK
DEFLAGRATION MODEL

SA-4770-14

65
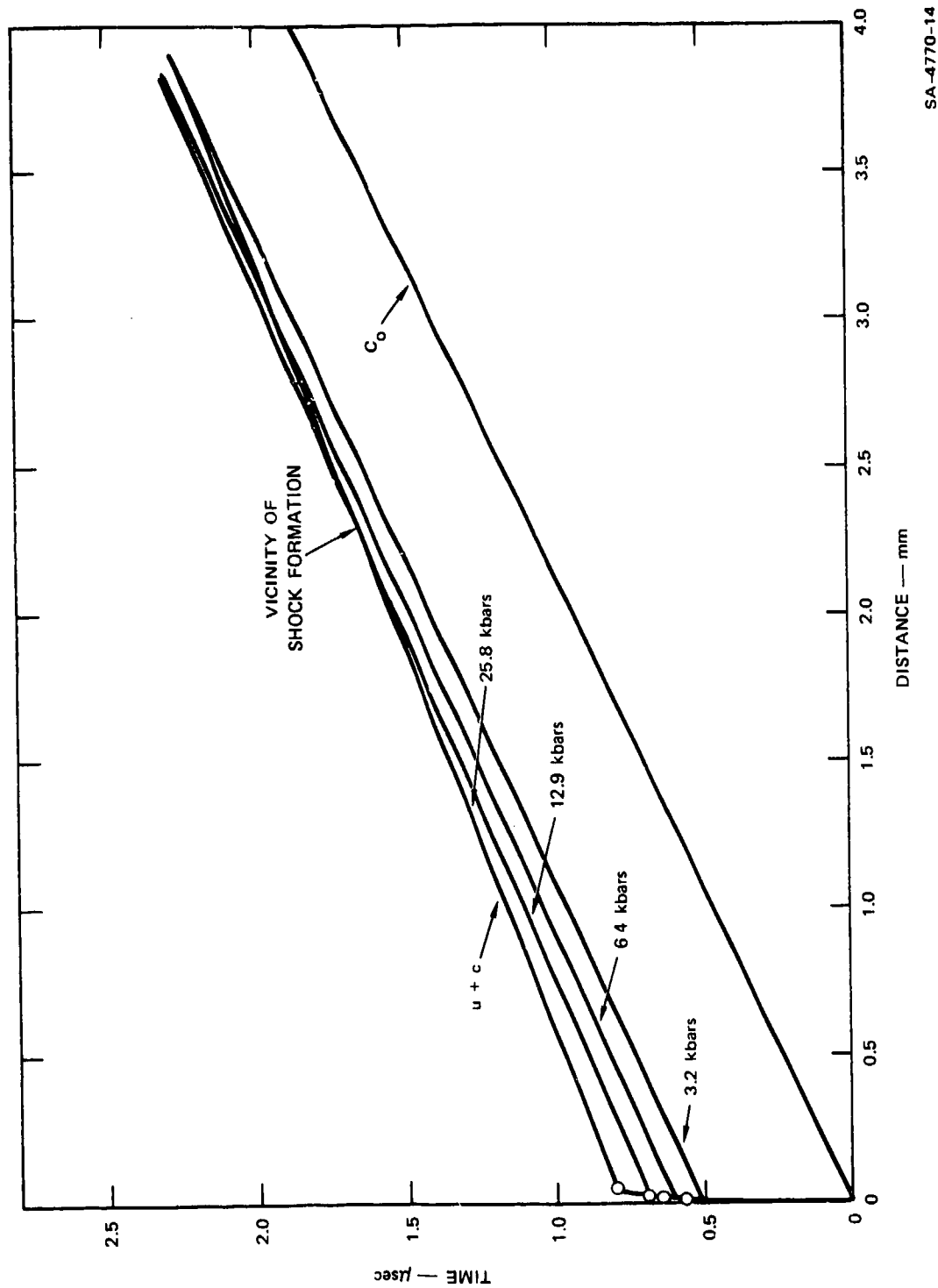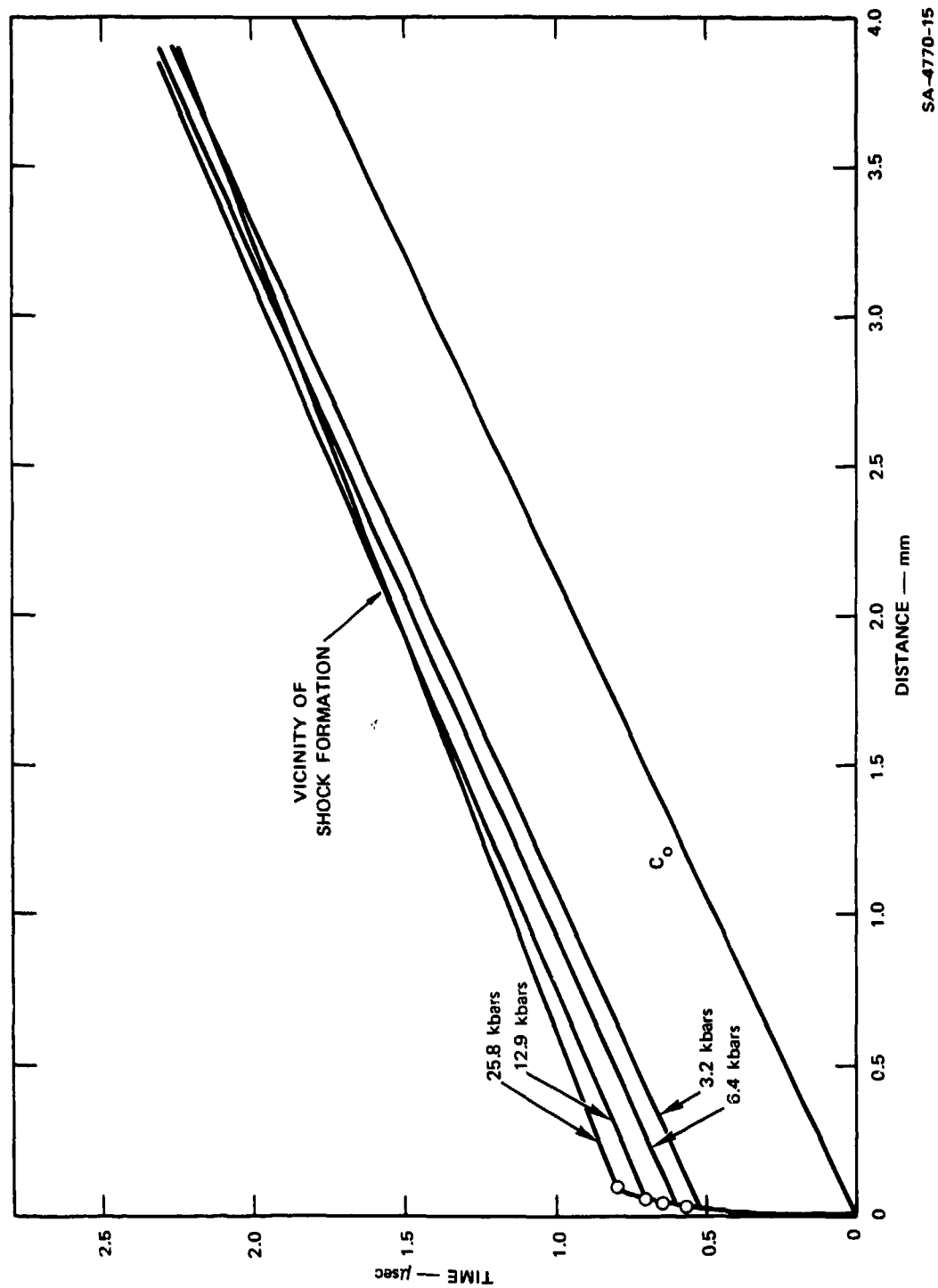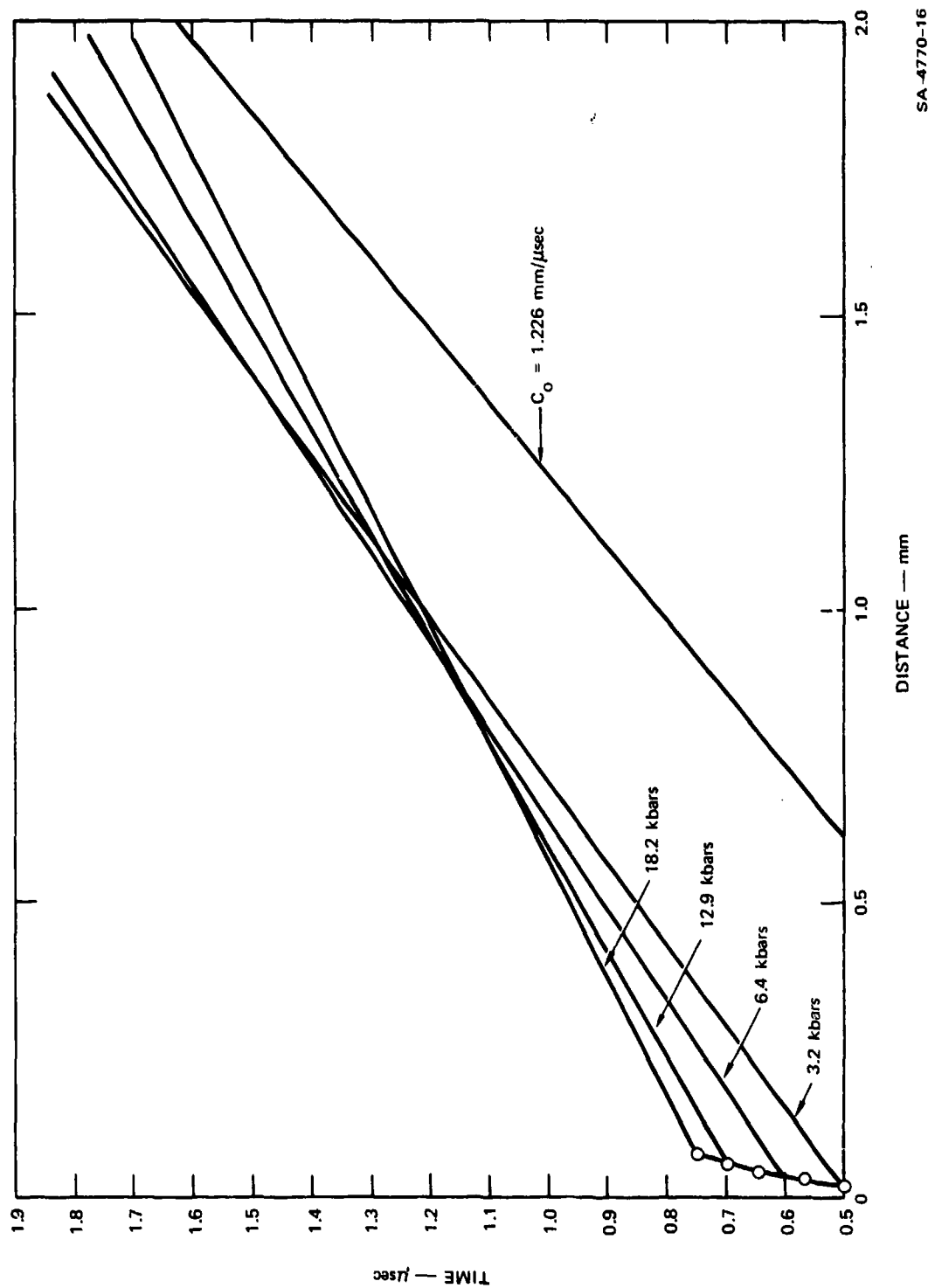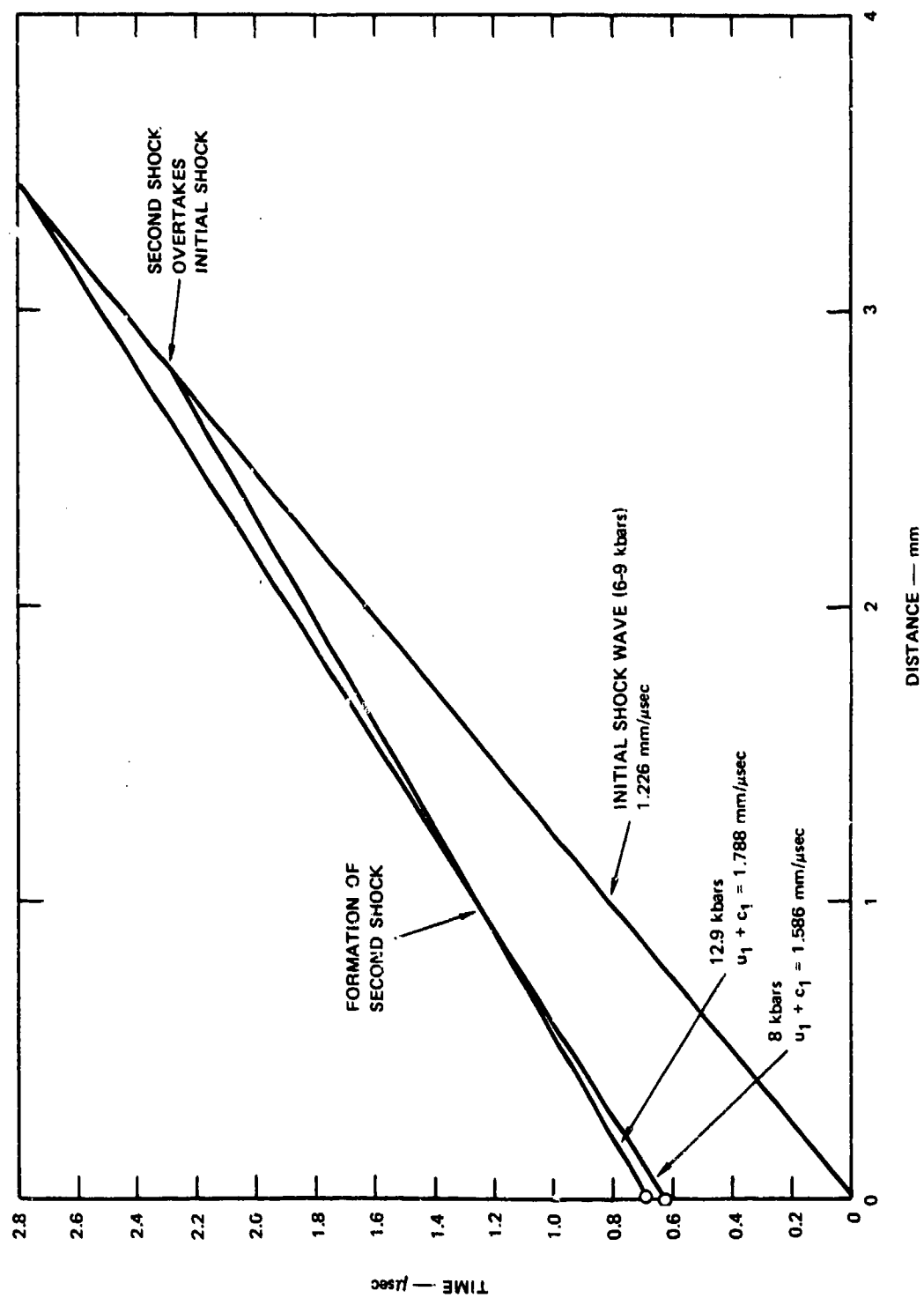
FIGURE 18   DISTANCE-TIME DIAGRAM FOR DDT IN α-LEAD AZIDE CRYSTALS USING A CJ DEFLAGRATION MODEL

SA-4770-15

66

FIGURE 19   DISTANCE-TIME DIAGRAM FOR DDT IN PRESSED LEAD AZIDE (ρ_o = 3.4 g/cc) USING A CJ DEFLAGRATION MODEL

SA-4770-16

67

FIGURE 20 DISTANCE-TIME DIAGRAM FOR SDT IN PRESSED LEAD AZIDE

68

calculation resulted in the formation of a second shock wave due to the crossing of the characteristics ahead of the flame. This second shock wave may cause detonation at 1.3 μsec and 1.1 mm, or detonation may result when the second shock overtakes the initial shock at 2.3 μsec and 2.8 mm. Some of Davies'[18] gage records did appear to detect two finite strength shocks at 1 or 2 mm into the explosive in tests where detonation occurred at 3 or 4 mm. Again the order of magnitude agreement between the SDT approach and Davies'[18] results is as good as can be expected at the present time.

From these DDT and SDT calculations on pentolite and lead azide, it is apparent that the experimental data on pressure-time histories in the deflagration region, on deflagration velocity, and on shock formation ahead of the flame are scarce and poor. Thus a good test of the modified Macek approach to DDT cannot be made on primaries or secondaries. Well-instrumented DDT experiments on primary explosives are critically needed to provide a first step toward an understanding of DDT in primaries. Experiments using stress gages and wave velocity measurement techniques during DDT in cast 2-MNT and other primaries are suitable for providing precise pressure and velocity data to use in further development of the theory.

IV CONCLUSIONS

During the last period of the contract series, we determined the
threshold voltages for initiation of cast 1-MNT and 2-MNT. The time for
DDT as a function of charge length was measured for cast 2-MNT. Two
analytical models of deflagration were incorporated into Macek's theoreti-
cal description of DDT, resulting in improved calculations for DDT in
cast pentolite. These models were also tested to a limited extent on
the meager existing data on lead azide. In analyzing the experimental
work on DDT in cast secondaries, the lack of precise pressure and velocity
measurements was apparent.

In future research, precise measurements of pressure and wave
velocities should be made in the critical regions of cast primaries where
DDT develops. These measurements will give the first detailed results
of this type for cast primaries or secondaries. These data will furnish
the necessary input for a realistic test of the theoretical DDT approach.

The precise pressure measurements will entail the use of Lagrange
stress gages in an apparatus similar to the time-for-DDT measurement
apparatus. Three recent applications of these gages in explosives re-
search imply that their use in DDT of primaries will be successful. As
previously discussed, Davies et al.[18] successfully used manganin and
carbon stress gages in flyer plate impact SDT studies of pressed lead
azide. In recent gage development work at SRI, manganin stress gages
were used to measure detonator output at distances of a few millimeters
from an exploding bridgewire.[28] In DDT experiments only a heated bridge-
wire is used, so the bridgewire noise level should be even less of a
problem. Mangani. stress gages have also survived reactive shock pres-
sures of 60-80 kbar in shock initiation studies of cast TNT.[27] These

70

pressures are higher than the range of pressures to be measured during the DDT process, because the shock initiation threshold of a primary should be about 10-20 kilobars. Single crystals of lead azide have been initiated by thin flyer plates accelerated to velocities corresponding to 10-kbar pressures in the crystal.[36]

The stress gage experiments will measure stress histories in the deflagration zone near the bridgewire, in the transition zone where shock formation occurs, and in the detonation region. Although pressure measurements in the region of the CJ state are not feasible at this time, pressures of 60-80 kilobars would certainly indicate that detonation will occur. The deflagration velocities near the bridgewire will also be monitored to determine whether the high velocities predicted by our analytical models are reached and, if these velocities are reached, which of the two models (Adams-Pack or CJ deflagration) predicts the velocity more accurately. The experiments will be carried out on cast 2-MNT and cast 1-MNT to determine the difference in pressure histories that makes 2-MNT a much better primary than 1-MNT. They may also be carried out on other available primaries, such as pressed lead azide. The pressure and deflagration velocity histories will also provide the input data for a valid test of the theoretical description of DDT in cast explosives.

Once the DDT aspect of primary explosives is quantified, the main emphasis of the research program can be placed on determining the structural properties that control the pressure-time and deflagration velocity-time histories. An understanding of these histories from a chemical kinetics point of view is the next step in understanding the action of primary explosives. This step is a difficult one to take, however. One possible approach, for primaries like lead azide that decompose into simple reaction product mixtures (Pb and N_2), would be to calculate the rate of uni-molecular decomposition from the measured pressure history behind the

71

deflagration wave. The measured deflagration velocity history and pressure history in the unreacted explosive would determine the pressure drop across the deflagration zone. A realistic equation of state for the compressed unreacted explosive ahead of the flame front would complete the thermo-dynamic description of the primary explosive as a function of time and distance. This thermodynamic description would be incorporated into a chemical kinetic model of unimolecular decomposition that is consistent with the experimental results. A similar derivation of a chemical kinetic model for decomposition of a more complex molecule containing C, H, O, and N atoms, such as 2-MNT, would require assumptions about the sequence of intermediate reactions involved in the decomposition process. It would also be important to explain the measured deflagration velocity history using the theory of conductive flames and to calculate the energy release rate within the deflagration zone.

The final step in developing a useful correlation between chemical structure and primary explosive behavior is to relate chemical kinetics to chemical structure. This type of relationship between kinetics and structure has been developed on a qualitative basis for many chemical systems, including liquid secondary explosives.[40] These qualitative relationships have proven useful for certain applications of secondary explosives. A logical approach for primary explosives is to develop qualitative relationships between the chemical kinetic models that are consistent with DDT experimental results and the chemical structures of various types of primaries. These qualitative relationships may provide sufficient guidelines for producing better primaries. However, because of the complex and varied nature of primary explosives, it may be necessary to generate a great deal of experimental DDT and kinetic data. These data would serve as the required base for formulating detailed quantitative relationships between chemical kinetics and structure, which include con-tributions from all groups present in the molecule, that may be necessary to explain the effects of structure on primary explosive performance.

REFERENCES

1. H. D. Fair and R. F. Walker, _Physics and Chemistry of the Inorganic Azides_, Vol. 1 (Plenum, New York, 1977). Other volumes are to follow.

2. (a) R. Shaw, "Structure/Property Correlations in Primary Explosives," SRI Technical Progress Report 74-2 (Annual), Project PYU-2842, Menlo Park, CA (December 1974);
   (b) J. M. Guimont, M. E. Hill, R. Shaw, and C. M. Tarver, "Structure/ Property Correlations in Primary Explosives," SRI Technical Progress Report 75-2 (Annual), Project PYU-3692, Menlo Park, CA (September 1975).

3. H. M. Peters, R. L. Simon, Jr., W. G. Blucher, D. L. Ross, and T. C. Goodale, "Synthesis and Testing of Primary Explosives," Final Report, Project PYU-2044, Menlo Park, CA (December 1972).

4. P. Gray, Proc. Roy. Soc. A 246, 202 (1958).

5. G.W.C. Taylor and J. M. Jenkins, personal communication, 1973.

6. R. Roberts, personal communication, 1973.

7. S. W. Benson and R. Shaw, unpublished work, 1974.

8. R. Reed, personal communication, 1974.

9. (a) C. L. Scott, Proceedings of the International Conference on Research in Primary Explosives (ERDE, Waltham Abbey, Essex, England, March 17-19, 1975) Vol. 2, paper 15;
   (b) W. H. Gilligan and M. J. Kamlet, _Synthesis of Mercuric 5- Nitrotetrazole_, NSWC/WOL/TR76-146 (December 9, 1976).

10. L. R. Bates and J. M. Jenkins, Proceedings of the International Conference on Research in Primary Explosives (ERDE, Waltham Abbey, Essex, England, March 17-19, 1975) Vol. 2, paper 12/14.

11. L. R. Bates and J. M. Jenkins, Proceedings of the International Conference on Research in Primary Explosives (ERDE, Waltham Abbey, Essex, England, March 17-19, 1975) Vol. 2, paper 12/5.

12. P. J. Haskins, Proceedings of the International Conference on Research in Primary Explosives (ERDE, Waltham Abbey, Essex, England, March 17-19, 1975) Vol. 2, paper 14/21 and pages following.

13. H. A. Golopol, D. B. Fields and G. L. Moody, "A New Booster Explosive, LX-15," UCRL-52175, Rev. 1, March 18, 1977.

14. A. Macek, J. Chem. Phys. 31, 162 (1959).

15. R. R. Bernecker and D. Price, Combust. Flame 22, 161 (1974).

16. H. S. Leopold, "A New Technique for Detecting the Initial Reaction o of Primary Explosives Initiated by Hot Wire," NOLTR 69-148, November 7, 1969.

17. R. A. Henry and W. G. Finnigan, J. Amer. Chem. Soc. 76, 923 (1954).

18. F. W. Davies, A. B. Zimmershied, F. G. Borgardt, and L. Avrami, J. Chem. Phys. 64, 2295 (1976).

19. M. M. Chaudhri and J. E. Field, Fifth Symposium (International) on Detonation, Office of Naval Research, ARC-184, Pasadena, CA (1970), p. 301.

20. G. B. Kistiakowsky, Third Symposium on Combustion, Flame, and Explosion Phenomena (Williams and Wilkins, Baltimore, Maryland, 1949), p. 560.

21. A. R. Ubbeholde, Third Symposium on Combustion, Flame, and Explosion Phenomena (Williams and Wilkins, Baltimore Maryland, 1949), p. 566.

22. R. W. Gibson and A. Macek, Eighth Symposium (International) on Combustion, (Williams and Wilkins, Baltimore, Maryland, 1962), p. 847.

23. C. T. Zovko and A. Macek, Third Symposium (International) on Detonation, Office of Naval Research (1960), p. 606

24. A. Macek, Chem. Rev. 62, 41 (1962).

25. R. Courant and F. O. Friedricks, Supersonic Flow and Shock Waves (Interscience Publishers, Inc., New York, 1948), p. 87.

26. K. K. Andreev and S. V. Chuiko, Russian J. Phys. Chem. 37, 695 (1963).

27. M. Cowperthwaite and J. T. Rosenberg, private communication.

28. J. T. Rosenberg and D. F. Walter, "Development of Two Improved Output Tests and Detonator-Detonating Fuze Devices," SRI Final Report on Project PYU-2691, Menlo Park, CA (May 1974).

29. S. J. Jacobs, private communication.

30. Ya. B. Zel'dovich and A. S. Kompaneets, Theory of Detonation (Academic Press, New York, 1960), p. 112.

31. J. Taylor, Detonation in Condensed Explosives (Clarendon Press, Oxford, 1952), Chapter VI.

32. B. Lewis and G. Von Elbe, Combustion, Flames and Explosions of Gases (Academic Press, New York, 1960), Chapter V.

33. G. K. Adams and D. C. Pack, Seventh Symposium (International) on Combustion (Butterworths, London, 1959), p. 812.

34. Ya. K. Troshin, Seventh Symposium (International) on Combustion (Buterworths, London, 1959), p. 789.

35. D. Price and J. F. Wehner, Combust. Flame $\underline{9}$, 73 (1965).

36. M. M. Chaudhri, Combust. Flame $\underline{19}$, 419 (1972).

37. W. E. Deal, J. Chem. Phys. $\underline{27}$, 796 (1957).

38. H. S. Leopold, "The Growth to Detonation of Binary Explosive Mixtures," NOLTR63-129 (April 16, 1963).

39. N. Slagg, private communication to Robert Shaw, 1974.

40. M. E. Hill, T. Mill, D. S. Ross, R. Shaw, R. W. Woolfolk, and C. Tarver, "Sensitivity Fundamentals," SRI Technical Progress Report 73-3 (Semiannual), Project PYU-8525, Menlo Park, CA (December 1973).

Appendix A

SYNTHESES OF 1- AND 2-METHYL-5-NITROTETRAZOLES

The procedures described below were used to synthesize 1- and 2-methyl-5-nitrotetrazole for use in the measurements of deflagration to detonation transitions of these cast primaries.

1-Methyl-5-Nitrotetrazole

A mixture of 50 g of aminotetrazole monohydrate, 19.1 g of sodium hydroxide, and 97 ml of water was heated to 92-95°C, and 31.7 g of dimethyl sulfate was added dropwise over 40 minutes. The temperature of the reaction mixture was held at 95°C for an additional hour and then cooled to 5°C overnight. The product, 1-methyl-5-aminotetrazole, was removed by filtration, washed with cold water, and dried to yield 24.2 g. This synthesis was developed by Henry and Finnegan.[1]

A mixture of 5 g of 1-methyl-5-aminotetrazole from above, 17 ml of 96% sulfuric acid, and 300 ml of water was added dropwise over 1 hour to a solution of 53 g of sodium nitrite in 500 ml of water at 45°C. The reaction mixture was stirred an additional hour at 45°C and then cooled to 25°C. The reaction was extracted with three 50-ml portions of methylene chloride. The methylene chloride extract was washed once with 5% sodium bicarbonate and once with water. It was dried over magnesium sulfate and evaporated, leaving 1.5 g of yellow oil. This was combined with 6.0 g of oil from another reaction and dissolved in a minimum volume of diethyl ether. The ether solution was passed through a neutral

---

[1] R. Henry and W. Finnegan, J. Amer. Chem. Soc. **76**, 923 (1954).

alumina column. The product from the column was recrystallized twice from ether to yield 3.5 g of 1-methyl-5-nitrotetrazole, mp 52°C. No trace of nitrosamine could be detected by infrared analysis. The product, 1-1-methyl-5-nitrotetrazole, was stored in methylene chloride solution at 0°C in the dark. This synthesis procedure was developed by Bagal et al.[2]

2-Methyl-5-Nitrotetrazole

A mixture of 50 g of aminotetrazole monohydrate, 15 ml of 96% H_2SO_4, and 970 ml of water was added over 45 min to a mixture of 77.7 g of sodium nitrite, 48.5 g of copper sulfate, and 730 ml of water. The temperature was allowed to rise slowly from 0° to 25°C during the addition period. The reaction mixture was stirred an additional 2 hours until nitrogen evolution had stopped. Concentrated sulfuric acid, 44 ml, was added and the mixture was cooled to 5°C. The product, copper 5-nitrotetrazole, was removed by filtration and washed with water. This procedure was developed by von Herz[3a] and has been modified by Gilligan and Kamlet.[3b]

The copper salt from above was dissolved in boiling water, and a sodium hydroxide solution was added slowly until the pH was ~ 9. After boiling for 30 min more, the mixture was cooled to 25°C and filtered to remove the copper oxide. The filtrate was concentrated and cooled to 5°C. The crystallized sodium salt was removed by filtration and air dried to yield 35 g. This procedure was developed by von Herz.[3a]

---

[2]L. I. Bagal, et al., Khim. Geterotsikl., Soedin. (1970), p. 259; Chem. Abstracts 72, 111383h.

[3a]E. von Herz, U.S. Patent 2,066,954 (1937); [b]W. H. Gilligan and M. J. Kamlet, "Synthesis of Mercuric 5-Nitrotetrazole," NSWC/WOL/TR 76-146 (6 December 1976).

A mixture of 18 g of sodium 5-nitrotetrazole tetrahydrate from above, 400 ml of water, 160 ml of acetone, and 20 g of methyl iodide was refluxed for 3.5 hr. More methyl iodide, 6 g, was added after the first 2 r. The acetone was removed by distillation, and 400 ml of benzene was added. The mixture was then washed with 100 ml of 2% sodium hydroxide in brine. After two additional washings with 25-ml portions of brine, the solution was dried over magnesium sulfate and evaporated to dryness. The residue was dissolved in a mixture of 200 ml of benzene and 60 ml of petroleum ether and cooled to 0°C for 24 hr. The product was removed by filtration and dried under vacuum. Yield was 4.8 g, mp 85°C. The product, 2-methyl-5-nitrotetrazole, was stored in methylene chloride solution at 0°C in the dark. This procedure was developed by Henry and Finnegan.[4]

---

[4]
R. Henry and W. Finnegan, J. Amer. Chem. Soc. 76, 923 (1954).

Appendix B

ESTIMATION OF HEATS OF FORMATION AND DENSITIES OF
1- and 2-METHYL-5-NITROTETRAZOLE

The use of additivity methods to estimate the heats of formation at 25°C of 1-methyl-5-nitrotetrazole (1-MNT), 2-methyl-5-nitrotetrazole (2-MNT), and for comparison, 5-azidotetrazole (5AZT) is described below. All heats are in kcal/mole.

The heats of formation of 1-MNT and 2-MNT were obtained by estimating the effect of adding methyl groups to 5-nitrotetrazole (TNO_2) at the 1- and 2-positions. The heat of formation of TNO_2 was obtained by assuming that the difference in the heats of formation of TNO_2 and nitrobenzene ($PhNO_2$) is the same as the average difference in heats of formation of tetrazole compounds (TX) substituted at the 5-position and phenyl compounds wit' the same substituents (PhX). That is, the basic assumption is that

$$\Delta H_f(TNO_2) - \Delta H_f(PhNO_2) = \Delta H_f(TX) - \Delta H_f(PhX) \qquad (B-1)$$

The values for tetrazole compounds were obtained from the work of Domalski;[1] the values for phenyl compounds are from Cox and Pilcher.[2] The average value of $\lceil \Delta H_f(TX) - \Delta H_F(PhX) \rceil$ was calculated as shown in Table B-1.

---

[1] E. S. Domalski, J. Phys. Chem. Ref. Data 1, 221 (1972).

[2] J. D. Cox and G. Pilcher, Thermochemistry of Organic and Organometallic Compounds (Academic Press, New York, 1970).

81

Table B-1

COMPARISON OF THE HEATS OF FORMATION OF
DERIVATIVES OF TETRAZOLE AND BENZENE

X	Tetrazole Derivatives TX (all solid)	Benzene Derivatives PhX (all ideal gas)	Δ(TX - PhX)
H	56.7	19.8	36.9
OH	1.5	-23.0	24.5
NH_2	49.7	20.8	28.9
CN	96.1	51.5	44.6
CH_3O	16.6	-17.3	33.9

Average 34 ± 10

Inserting the average value for ΔH_f(TX, solid) minus ΔH_f(PhX, ideal gas) into equation (B-1) gave

$$\Delta H_f(TNO_2, \text{ solid}) - \Delta H_f(PhNO_2, \text{ ideal gas}) = 34 \qquad \text{(B-2)}$$

A value of 16.9 kcal/mol for ΔH_f(PhNO$_2$), from previous work,[3] was used to give:

$$\Delta H_f(TNO_2, \text{ solid}) = 34 + 16.9 = 51 \qquad \text{(B-3)}$$

The effect of adding methyl groups to TNO$_2$ at the 1- and 2-positions to form 1MNT and 2MNT was estimated by comparing 5-aminotetrazole (AT) with 1- and 2-methyl-5-aminotetrazole (LMAT and 2MAT). That is, we assumed that

$$\Delta H_f(1MNT) - \Delta H_f(TNO_2) = \Delta H_f(1MAT) - \Delta H_f(AT) \qquad \text{(B-4)}$$

---

[3] R. Shaw, J. Phys. Chem. 75, 4046 (1971).

82

and that

$$\Delta H_f(2MNT) - \Delta H_f(TNO_2) = \Delta H_f(2MAT) - \Delta H_f(AT) \qquad \text{(B-5)}$$

Domalski's values[1] for $\Delta H_f(1MAT)$ and $\Delta H_f(AT)$ were used in equation (4) to give:

$$\Delta H_f(1MNT) = \Delta H_f(1MAT) - \Delta H_f(AT) + \Delta H_f(TNO_2) \qquad \text{(B-6)}$$

$$= 46.2 - 49.7 + 51 = 48.5$$

Rounding off, $\Delta H_f(1MNT) = 48$.

From equation (B-5) and Domalski's values,[1]

$$\Delta H_f(2MNT) = \Delta H_f(2MAT) - \Delta H_f(AT) + \Delta H_f(TNO_2) \qquad \text{(B-7)}$$

$$= 50.4 - 49.7 + 51$$

$$= 51.7$$

Rounding off, $\Delta H_f(2M) = 52$.

The heat of formation of 5-azidotetrazole (5AZT) was obtained from the assumption that ΔH_f(5-azidotetrazole, solid) minus ΔH_f(tetrazole, solid) is equal to ΔH_f(cyclopentane azide, ideal gas) minus ΔH_f(cyclopentane, ideal gas):

$$\Delta H_f(5AZT) - \Delta H_f(CH_2N_4) = \Delta H_f(C_5H_9N_3) - \Delta H_f(C_5H_{10}) \qquad \text{(B-8)}$$

We inserted the values of Cox and Pilcher[2] for $\Delta H_f(C_5H_9N_3)$ and $\Delta H_f(C_5H_{10})$ and Domalski's value[1] for $\Delta H_f(CH_2N_4)$ into equation (B-8) to obtain

$$\Delta H_f(5AZT) = \Delta H_f(C_5H_9N_3) - \Delta H_f(C_5H_{10}) + \Delta H_f(CH_2N_4) \qquad \text{(B-9)}$$

$$= 52.8 + 18.4 + 56.7 = 127.9$$

Rounding off, $\Delta H_f(5AZT) = 128$.

83

Additivity methods were also used to estimate the density of 1MNT
The density is found by dividing the molecular weight by the molar volume.
The molar volumes given in Table B-2 show that the difference between the
molar volumes of the 2-isomer and the 1-isomer of allytetrazole (in the
liquid state at 20°C) is very similar to the difference between the
molar volumes of the 2-isomer and the 1-isomer of vinyltetrazole (also
in the liquid state at 20°C). These values of 3.4 and 3.5 cm^3/mol are
within experimental error of each other. Furthermore, the slight change
in the physical state for the other pairs of isomers, namely, the liquid
state at 25°C and the solid state, changes the difference by less than
2% of the average molar volumes to 4.3 and 4.9 cm^3/mol. Therefore it
ought to be a very good approximation that the difference between molar
volumes of the 2-isomer and the 1-isomer for all tetrazoles in the solid
state is 4.9 cm^3/mol.

From the known molar volume of 70.1 cm^3/mol for 2MNT, the molar volume
of 1MNT = 70.1 - 4.9 = 65.2 cm^3/mol. The density of 1MNT is therefore
115/65.2 = 1.76 g/cm^3.

DISTRIBUTION LIST

Quantity	Destination
Sixteen (16)	Department of the Navy Naval Sea Systems Command Washington, D.C. 20362 (N00017) Attn: Code SEA-0332 (2) Code SEA-0623 (13) includes DDC Code SEA-992E (1)
One (1)	Department of the Navy Naval Sea Systems Command Washington, D.C. 20362 Attn: Code SEA-0332 VIA: Chief, Defense Contract Administration Services Region, San Francisco 866 Malcolm Road Burlingame, CA 94010 (S0507A)
One (1)	Commanding General U.S. Army Materiel Command Washington, D.C. 20315 (DAAG01) Attn: Library
Two (2)	Commanding Officer U.S. Army Picatinny Arsenal Dover, New Jersey 07801 (DAA21) Attn: SARPA-FR-E-C (1) Technical Library (1)
One (1)	Commanding General U.S. Army Combat Developments Command Fort Belvoir, VA 22060 (DAAK02)
Three (3)	Commander, Naval Air Systems Command Washington, D.C. 20360 (N00019) Attn: Code AIR-03 (1) Code AIR-350 (1) Code AIR-604 (1)
Three (3)	Commander, Naval Surface Weapons Center/WOL Silver Spring, MD 20910 (N60921) Attn: Dr. J. Enig (1) Dr. S. J. Jacobs (1) Technical Library (1)

One (1)	Commanding Officer Naval Weapons Station Yorktown, VA 23491 (N00109) Attn: NEDED
One (1)	Commanding Officer Naval Ordnance Station Indian Head, MD 20640 (N00174) Attn: Technical Library
Three (3)	Commander Naval Weapons Center China Lake, CA 93555 (N60530) Attn: Code 753 (2) Code 454 (1)
One (1)	Commander Naval Surface Weapons Center/DL Dahlgren, VA 22448 (N00178) Attn: Technical Library
Two (2)	Air Force Systems Command (AFSC) Andrews Air Force Base Washington, D.C. 20390 (F18600) Attn: SCSM (1) SCT (1)
One (1)	Director Advanced Projects Research Agency Department of Defense Washington, D.C. 20301